Iridium Olefin Complexes Bearing Dialkylamino/amido PNP Pincer Ligands: Synthesis, Reactivity, and Solution Dynamics†

Anja Friedrich, Rajshekhar Ghosh, Roman Kolb, Eberhardt Herdtweck, and Sven Schneider*

Department Chemie, Technische Universität München, Lichtenbergstrasse 4, D-85747 Garching b. München, Germany

Received May 9, 2008

The reaction of $[IrCl(COE)_2]_2$ (**1**, COE = cyclooctene) with pincer ligand $HN(CH_2CH_2P^iPr_2)_2$ ($(PNP)^H$) and $AgPF_6$ gives iridium(I) amino olefin complex $[Ir(COE)(PNP)^H]PF_6$ ($\mathbf{3^{COE}\text{-}PF_6}$). Without anion exchange, the stability of $\mathbf{3^{COE}\text{-}Cl}$ is highly solvent dependent. In benzene or THF a mixture of amido complex [Ir(COE)(PNP)] ($\mathbf{4^{COE}}$), $[IrHCl_2(PNP)^H]$ (**5**), and $[IrHCl(C_8H_{13})(PNP)^H]$ (**6**) with a vinylic cyclooctenyl ligand is obtained. A pathway is proposed that includes concurrent trapping of intramolecular C−H versus intermolecular N−H activation products. $\mathbf{3^L\text{-}PF_6}$ (L = C_2H_4, C_3H_6, CO) are prepared by olefin substitution. Deprotonation with KO^{t}Bu gives the corresponding amido complexes [IrL(PNP)] ($\mathbf{4^L}$; L = COE, C_2H_4, CO). Reversible COE C−H activation is proposed to account for the fluxional behavior of $\mathbf{3^{COE}\text{-}PF_6}$ in solution as compared with the structural rigidity of $\mathbf{4^{COE}}$, which points toward strong N→Ir π-donation in the amido complexes.

Introduction

In the past years, late transition metal complexes bearing pincer ligands have been utilized in numerous stoichiometric and catalytic reactions, such as Heck coupling,[1] alkane dehydrogenation,[2] N−H activation,[3] or olefin hydroamination.[4,5] With group 9 metals, particularly diphosphino pincers have proven to be effective ligands supporting intermolecular C−H activation reactions.[2,6] Recently, Krogh-Jespersen et al. examined theoretically and experimentally the thermodynamics of RH (R = H, aryl, alkyl) oxidative addition to (*p*-R′-PCP)IrL (*p*-R′-PCP = 4-R′-C_6H_2-2,6-$(CH_2PR''_2)_2$; L = no ligand, CO, H_2), rationalizing the results in terms of C_{PCP}−Ir MO interactions.[7] Variation of the *para* aryl substituent R′ showed that RH addition to the parent (*p*-R′-PCP)Ir fragment is favored by increasing C_{PCP}→Ir π-donation due to a destabilizing filled−filled C_{PCP}−Ir repulsion. However, the influence of strongly π-donating auxiliary ligands, such as amides, on C−H bond activation reactions is not well examined. Ozerov and co-workers have recently studied halobenzene C−H and C−X oxidative addition to the diarylamido pincer fragment (PNP′)Ir (PNP′ = $N(C_6H_3$−4-Me-2-$P^iPr_2)_2$; Figure 1, **B**).[6a] Milstein and co-workers have demonstrated, that the backbone methylene groups of pyridine-based pincer complex $[(PNP^*)Ir(COE)]^+$ (PNP^* = C_5H_3N-$(CH_2P^tBu_2)_2$; COE = cyclooctene) can be reversibly deprotonated. The resulting isolable amido complex adds benzene across the ligand backbone under mild conditions.[6c]

This example illustrates the utilization of a *cooperating ligand*, which undergoes reversible chemical transformations during the crucial bond activation steps.[8] In catalysis, this concept has been applied successfully to transfer hydrogenation of polar double bonds E═CRR′ (E = O, NR″), where the heterolytic activation of H_2 by Ru amido complexes was coined *bifunctional catalysis*.[9] Grützmacher and co-workers recently used iridium amido complexes for highly efficient transfer hydrogenation with benzochinone as hydrogen acceptor.[10] The proposed catalytic cycle comprises stepwise N−H deprotonation, one-electron oxidation, and H-transfer from the alcohol substrate and was therefore compared with the galactose oxidase catalyzed dehydrogenation of primary alcohols. Furthermore, they were able to isolate the oxidation product of a rhodium(I) amide, which was described as a metal-stabilized persistent aminoyl radical cation.[11]

† Dedicated to Prof. Dr. h.c. mult. W. A. Herrmann on the occasion of his 60th birthday.

* Corresponding author. E-mail: sven.schneider@ch.tum.de.

(1) (a) Ohff, M.; Ohff, A.; van der Boom, M. E.; Milstein, D. *J. Am. Chem. Soc.* **1997**, *119*, 11687.

(2) Goldman, A. S.; Renkema, K. B.; Czerw, M.; Krogh-Jespersen, K. In *Activation and Functionalization of C-H Bonds*; Goldberg, K. I., Goldman, A. S., Eds.; ACS Symposium Series 885; American Chemical Society: Washington, DC, 2004; pp 198−215.

(3) (a) Kanzelberger, M.; Zhang, X.; Emge, T. J.; Goldman, A. S.; Zhao, J.; Incarvito, C.; Hartwig, J. F. *J. Am. Chem. Soc.* **2003**, *125*, 13644. (b) Zhao, J.; Goldman, A. S.; Hartwig, J. F. *Science* **2005**, *307*, 1080. (c) Sykes, A. C.; White, P.; Brookhart, M. *Organometallics* **2006**, *25*, 1664. (d) Fafard, C. D.; Adhikari, D.; Foxman, B. M.; Mindiola, D. J.; Ozerov, O. V. *J. Am. Chem. Soc.* **2007**, *129*, 10318.

(4) (a) Michael, F. E.; Cochran, B. M. *J. Am. Chem. Soc.* **2006**, *128*, 4246. (b) Cochran, B. M.; Michael, F. E. *J. Am. Chem. Soc.* **2008**, *130*, 2786.

(5) van der Boom, M. E.; Milstein, D. *Chem. Rev.* **2003**, *103*, 1759.

(6) For recent examples see: (a) Fan, L.; Parkin, S.; Ozerov, O. V. *J. Am. Chem. Soc.* **2005**, *127*, 16772. (b) Feller, M.; Karton, A.; Leitus, G.; Martin, J. M. L.; Milstein, D. *J. Am. Chem. Soc.* **2006**, *128*, 12400. (c) Ben-Ari, E.; Leitus, G.; Shimon, L. J. W.; Milstein, D. *J. Am. Chem. Soc.* **2006**, *128*, 15390. (d) Kloek, S. M.; Heinekey, M.; Goldberg, K. I. *Organometallics* **2006**, *25*, 3007. (e) Whited, M. T.; Grubbs, M. T. *J. Am. Chem. Soc.* **2008**, *130*, 5874.

(7) Krogh-Jespersen, K.; Czerw, M.; Zhu, K.; Singh, B.; Kanzelberger, M.; Darji, N.; Achord, P. D.; Renkema, K. B.; Goldman, A. S. *J. Am. Chem. Soc.* **2002**, *124*, 10797.

(8) Grützmacher, H. *Angew. Chem.* **2008**, *120*, 1838; *Angew. Chem., Int. Ed.* **2008**, *47*, 1814.

(9) Noyori, R.; Ohkuma, T. *Angew. Chem.* **2001**, *113*, 40; *Angew. Chem., Int. Ed.* **2001**, *40*, 40. (b) Clapham, S. E.; Hadzovic, A.; Morris, R. H. *Coord. Chem. Rev.* **2004**, *248*, 2201. (c) Muniz, K. *Angew. Chem.* **2005**, *117*, 6780; *Angew. Chem., Int. Ed.* **2005**, *44*, 6622.

(10) Königsmann, M.; Donati, N.; Stein, D.; Schönberg, H.; Harmer, J.; Sreekanth, A.; Grützmacher, H. *Angew. Chem.* **2007**, *119*, 3637; *Angew. Chem., Int. Ed.* **2007**, *46*, 3567.

(11) Büttner, T.; Geier, J.; Frison, G.; Harmer, J.; Calle, C.; Schweiger, A.; Schönberg, H.; Grützmacher, H. *Science* **2005**, *307*, 235.

10.1021/om800423u CCC: $40.75
Publication on Web 01/14/2009

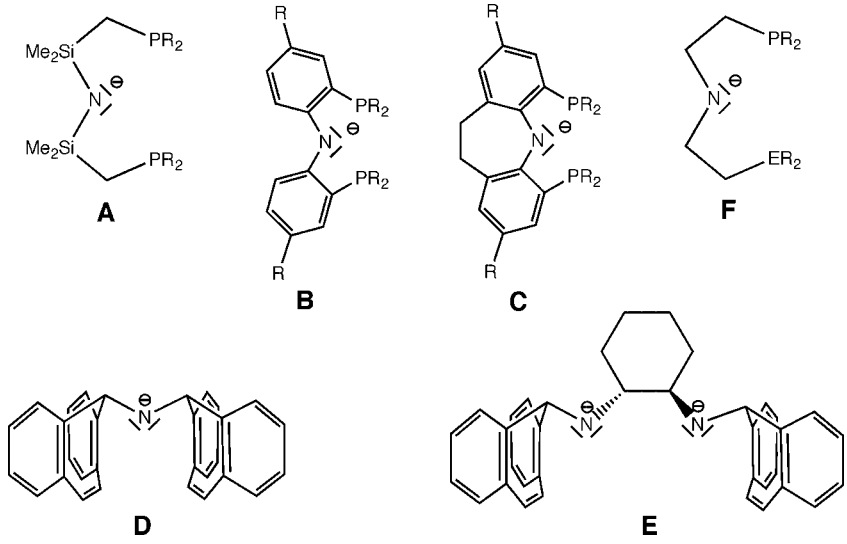

Figure 1. Amido chelate ligands used with group 9 metals.

Given this recent interest in late metal amido complexes for heterolytic and homolytic bond activation, the chemistry of group 9 amides is not well developed. Based on the pioneering work of Fryzuk,[12] Caulton described the synthesis of disilylamido complexes (Figure 1, **A**),[13] and Ozerov and co-workers utilized diarylamido pincers (Figure 1, **B** and **C**).[6a,14] However, complexes with more π-basic dialkylamido ligands are particularly scarce, presumably due to the intrinsic tendency to undergo β-H elimination.[15] Some rare examples are the rhodium and iridium complexes with biscycloheptatrienylamido- and biscycloheptatrienyldiamido-based chelate ligands developed by the Grützmacher group (Figure 1, **D** and **E**).[11,16] Recently, Abdur-Rashid, Gusev, and co-workers used bis(2-phophinoethyl)amido and 2-phosphinoethyl-2-aminoethylamido ligands to stabilize the iridium(III) amides [Ir(H)$_2$(PNP)] (PNP = N(CH$_2$CH$_2$P^{i}Pr$_2$)$_2$) and [Ir(H)$_2$(PNN)] (PNN = ^{i}Pr$_2$PCH$_2$CH$_2$NCH$_2$CH$_2$NEt$_2$) (**F**).[17] Both complexes are highly active catalysts for the transfer hydrogenation of ketones with 2-propanol and the postulated Noyori−Morris-type mechanism was recently confirmed in a theoretical examination.[18] However, no PNP iridium(I) complexes were reported.

In this article we describe the synthesis and reaction pathways toward a new class of iridium(I) amino and amido complexes bearing the pincer ligands HN(CH$_2$CH$_2$P^{i}Pr$_2$)$_2$ ((PNP)^H) and N(CH$_2$CH$_2$P^{i}Pr$_2$)$_2$ (PNP). Ligand N−H activation, vinylic olefin C−H activation, solution dynamics, and amino/amido bonding to the metal, which distinguish this ligand type from related diphosphine pincers, will be discussed.

Results

1. Reaction of [IrCl(COE)$_2$]$_2$ (1) with (PNP)^H: Solvent Influence. Clarke et al. reported that the reaction of [IrCl(COE)$_2$]$_2$ (**1**, COE = cyclooctene) with (PNP)^H in 2-propanol at 80 °C results in the formation of [Ir(H)$_2$Cl(PNP)^H] (**2**) (Scheme 1).[17a] However, monitoring the reaction of **1** with (PNP)^H in 2-propanol at room temperature by ^{31}P NMR spectroscopy we observed quantitative formation of iridium(I) amino olefin complex [Ir(COE)(PNP)^H]Cl (**3^{COE}-Cl**) by comparison with **3^{COE}-PF$_6$**, which was synthesized and fully characterized upon anion exchange (*vide infra*). To avoid hydride transfer from the solvent, the reaction was carried out in benzene, resulting in a 1:1 mixture of iridium(I) amido complex [Ir(COE)(PNP)] (**4^{COE}**) and iridium(III) hydride [IrHCl$_2$(PNP)^H] (**5**) (Scheme 1). Furthermore, C−H activation product [IrHCl(C$_8$H$_{13}$)(PNP)^H] (**6**) with a vinylic cyclooctenyl ligand was observed as a minor product in around 15% yield. **5** is easily isolated by extraction of **4^{COE}** and **6** with pentane. While **4^{COE}** was synthesized and fully characterized on another route (*vide infra*), **6** could not be isolated and was characterized from this mixture by multinuclear NMR.

2. Reaction of [IrCl(COE)$_2$]$_2$ (1) with (PNP)^H: Mechanistic Studies. Monitoring the reaction of **1** with (PNP)^H in C$_6$D$_6$ by ^{31}P and ^{1}H NMR reveals that multiple intermediates are formed over the course of 2 days at room temperature (Figure 2). As in 2-propanol, **3^{COE}-Cl** represents the first major intermediate. The large downfield ^{1}H chemical shift of the broad

(12) (a) Fryzuk, M. D.; MacNeil, P. A. *Organometallics* **1983**, *2*, 355. (b) Fryzuk, M. D.; MacNeil, P. A. *Organometallics* **1983**, *2*, 682. (c) Fryzuk, M. D.; MacNeil, P. A.; Rettig, S. J. *Organometallics* **1985**, *4*, 1145. (d) Fryzuk, M. D.; MacNeil, P. A.; Rettig, S. J. *J. Am. Chem. Soc.* **1985**, *107*, 6708. (e) Fryzuk, M. D.; MacNeil, P. A.; Rettig, S. J. *Organometallics* **1986**, *5*, 2469. (f) Fryzuk, M. D.; MacNeil, P. A.; McManus, N. T. *Organometallics* **1987**, *6*, 882. (g) Fryzuk, M. D.; MacNeil, P. A.; Rettig, S. J. *J. Am. Chem. Soc.* **1987**, *109*, 2803. (h) Fryzuk, M. D.; Bhangu, K. *J. Am. Chem. Soc.* **1988**, *110*, 961. (i) Fryzuk, M. D.; Huang, L.; McManus, N. T.; Paglia, P.; Rettig, S. J.; White, G. S. *Organometallics* **1992**, *11*, 1979. (j) Fryzuk, M. D.; Gao, X.; Joshi, K.; MacNeil, P. A.; Massey, R. L. *J. Am. Chem. Soc.* **1993**, *115*, 10581. (k) Fryzuk, M. D.; Gao, X.; Rettig, S. J. *J. Am. Chem. Soc.* **1995**, *117*, 3106.

(13) (a) Ingleson, M.; Fan, H.; Pink, M.; Tomaszewski, J.; Caulton, K. G. *J. Am. Chem. Soc.* **2006**, *128*, 1804. (b) Ingleson, M. J.; Fullmer, B. C.; Buschhorn, D. T.; Fan, H.; Pink, M.; Huffman, J. C.; Huffman, J. C.; Caulton, K. G. *Inorg. Chem.* **2008**, *47*, 407. (c) Verat, A. Y.; Pink, M.; Fan, H.; Tomaszewski, J.; Caulton, K. G. *Organometallics* **2008**, *27*, 166.

(14) (a) Ozerov, O. V.; Guo, C.; Papkov, V. A.; Foxman, B. M. *J. Am. Chem. Soc.* **2004**, *126*, 4792. (b) Weng, W.; Guo, C.; Moura, C.; Yang, L.; Fowman, B. M.; Ozerov, O. V. *Organometallics* **2005**, *24*, 3487. (c) Gatard, S.; Çelenligil-Çetin, R.; Foxman, B. M.; Ozerov, O. V. *J. Am. Chem. Soc.* **2006**, *128*, 2808.

(15) Bryndza, H. E.; Tam, W. *Chem. Rev.* **1988**, *88*, 1163.

(16) (a) Maire, P.; Büttner, T.; Breher, F.; Le Floch, P.; Grützmacher, H. *Angew. Chem.* **2005**, *117*, 6477; *Angew. Chem., Int. Ed*. **2005**, *44*, 6318. (b) Maire, P.; Breher, F.; Grützmacher, H. *Angew. Chem.* **2005**, *117*, 6483; *Angew. Chem., Int. Ed.* **2005**, *44*, 6325. (c) Maire, P.; Breher, F.; Schönberg, H.; Grützmacher, H. *Organometallics* **2005**, *24*, 3207. (d) Maire, P.; Königsmann, M.; Sreekanth, A.; Harmer, J.; Schweiger, A.; Grützmacher, H. *J. Am. Chem. Soc.* **2006**, *128*, 6578.

(17) (a) Clarke, Z. E.; Maragh, P. T.; Dasgupta, T. P.; Gusev, D. G.; Lough, A. J.; Abdur-Rashid, K. *Organometallics* **2006**, *25*, 4113. (b) Choualeb, A.; Lough, A. J.; Gusev, D. G. *Organometallics* **2007**, *26*, 5224.

(18) Bi, S.; Xie, Q.; Zhao, X.; Zhao, Y.; Kong, X. *J. Organomet. Chem.* **2008**, *693*, 633.

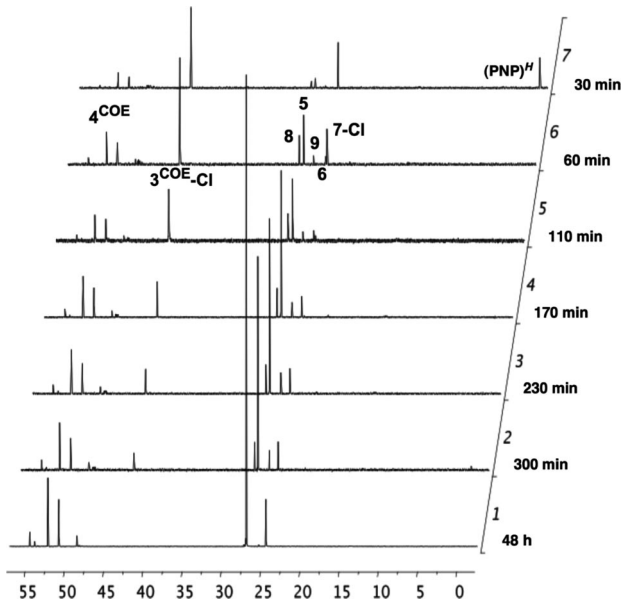

Figure 2. ^{31}P NMR spectra of the reaction of **1** with $(PNP)^H$ in C_6D_6.

Scheme 1. Reaction of $[IrCl(COE)_2]_2$ (1) with $HN(CH_2CH_2P^iPr_2)_2$ $(PNP)^H$ in 2-Propanol[17a] and Benzene, Respectively

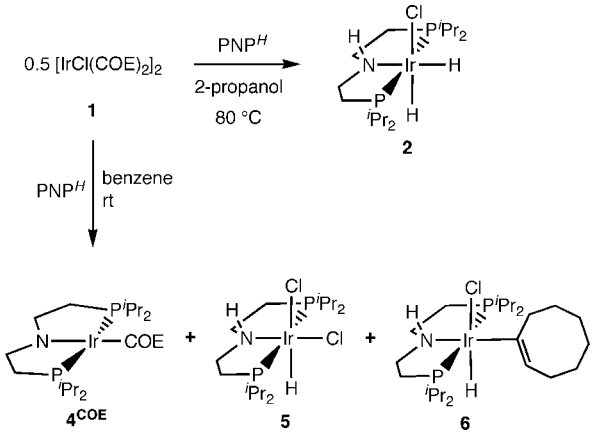

signal assigned to the N−H proton in **3^{COE}-Cl** (9.57 ppm/C_6D_6) relative to **3^{COE}-PF$_6$** (4.72 ppm/C_6D_6) indicates hydrogen bonding, presumably to the chloride counteranion. $[IrHCl(COE)(PNP)^H]Cl$ (**7-Cl**) is observed as an intermediate in an early stage of the reaction sequence, decaying quickly. Two further intermediates, **8** and **9**, that could not be prepared independently are observed by NMR.[19] However, the ^{1}H NMR spectrum of **8** strongly resembles complex **6**, indicating a vinylic cyclooctenyl ligand. On the other hand, between 3.5 and 8 ppm **9** features only a signal assignable to an N−H proton. The ^{1}H NMR signals for the hydride ligands of **8** (−23.39 ppm) and **9** (−23.66 ppm) are very close to each other and slightly downfield from **5** (−24.73 ppm) and **6** (−24.40 ppm). Therefore, we tentatively assign **8** and **9** to structures that are isomers of the final products **6** and **5**, respectively, with the hydride ligands in **8** and **9** in *trans* position to the $(PNP)^H$ amine donor and not *trans* to a chloride ligand as in **5** and **6**.

(19) Selected NMR data of **8** (C_6D_6, rt, [ppm]): ^{1}H NMR (399.78 MHz) δ−23.39 (t, $^2J_{HP}$ = 14.4 Hz, 1H, Ir-*H*), 2.94 (t, $^3J_{HH}$ = 5.5 Hz, 2H, IrCC*H*$_2$), 3.83 (br, 1H, N*H*), 6.27 (t, $^3J_{HH}$ = 8.6 Hz, 1H, =C*H*). ^{31}P{^{1}H} NMR (161.8 MHz): δ 25.8 (s, P^{i}Pr$_2$). Selected NMR data of **9** (C_6D_6, rt, [ppm]): ^{1}H NMR (399.78 MHz): δ−23.66 (t, $^2J_{HP}$ = 13.6 Hz, 1H, Ir-H), 6.36 (br, 1H, N*H*). ^{31}P{^{1}H} NMR (161.8 MHz): δ 27.7 (s, P^{i}Pr$_2$).

Scheme 2. Proposed Pathway for the Formation of 4^{COE}, 5, and 6 from 3^{COE}-Cl (iridium species are not fully characterized)

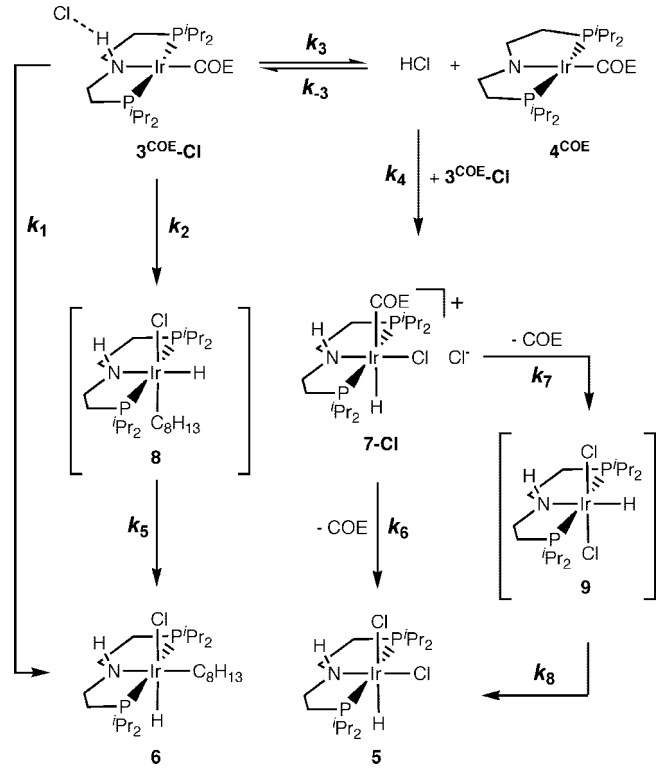

These results show that **3^{COE}-Cl** is initially formed in the reaction of **1** with $(PNP)^H$, but is not stable in nonprotic solvents, such as benzene or THF, slowly reacting toward **4^{COE}**, **5**, and **6**. Accordingly, **3^{COE}-PF$_6$** reacts with chloride sources such as $[PPh_4]Cl$ or $[N^nBu_3(CH_2Ph)]Cl$ in C_6H_6 or THF to give an equimolar amount of **4^{COE}** and **5** in combination with cyclooctenyl complex **6**, the latter in a slightly higher yield (approximately 20%). Based on the intermediates found for this reaction a pathway is proposed (Scheme 2).

To check for the viability of the model in Scheme 2, the kinetics of the reaction of **3^{COE}-PF$_6$** with chloride were studied by ^{31}P NMR spectroscopy. Kinetic experiments were conducted at 295 and 300 K in THF due to a lack of a suitable water-free chloride source that was soluble enough in benzene at the initial concentration $[\mathbf{3^{COE}\text{-}PF_6}]_0$ = 57.7 mM, and even in THF the equimolar amount of $[N^nBu_3(CH_2Ph)]Cl$ was not fully soluble.[20] However, plots of ln $[\mathbf{3^{COE}\text{-}PF_6}]$ versus time (Figure 3) were linear over three half-lifes with k_{obs} at 3.2 × 10^{-3} min^{-1} (298 K) and 4.5 × 10^{-3} min^{-1} (300 K), indicating that preequilibria such as dissolution of $[N^nBu_3(CH_2Ph)]Cl$ or formation of a **3^{COE}-Cl** precomplex are fast versus the decay of **3^{COE}-Cl**. Addition of COE did not affect k_{obs}. The concentrations of **3^{COE}-Cl**, **4^{COE}**, **5**, **6**, **7-Cl**, **8**, and **9** were fitted to the model outlined in Scheme 2 featuring a reasonable correlation of the simulation with experimental results (Figure 3 and Supporting Information).

3. Syntheses of Stable Iridium PNP Complexes. The reaction of **1** with $(PNP)^H$ in the presence of $AgPF_6$ or $NaBPh_4$ gives $[Ir(COE)(PNP)^H]X$ (**3^{COE}-X**; X = PF_6, BPh_4), which are stable in organic solvents (Scheme 3). Likewise, olefin complexes $[Ir(L)(PNP)^H]X$ (L = C_2H_4 (**3^{C2H4}-X**), C_3H_6 (**3^{C3H6}-X**); X = PF_6, BPh_4) can be prepared upon *in situ* olefin exchange in high yield. Facile substitution of ethylene versus CO gives

(20) The solubility of $[N^nBu_3CH_2Ph]Cl$ in d_8-THF at 295 K was derived by NMR spectroscopy (10 mM).

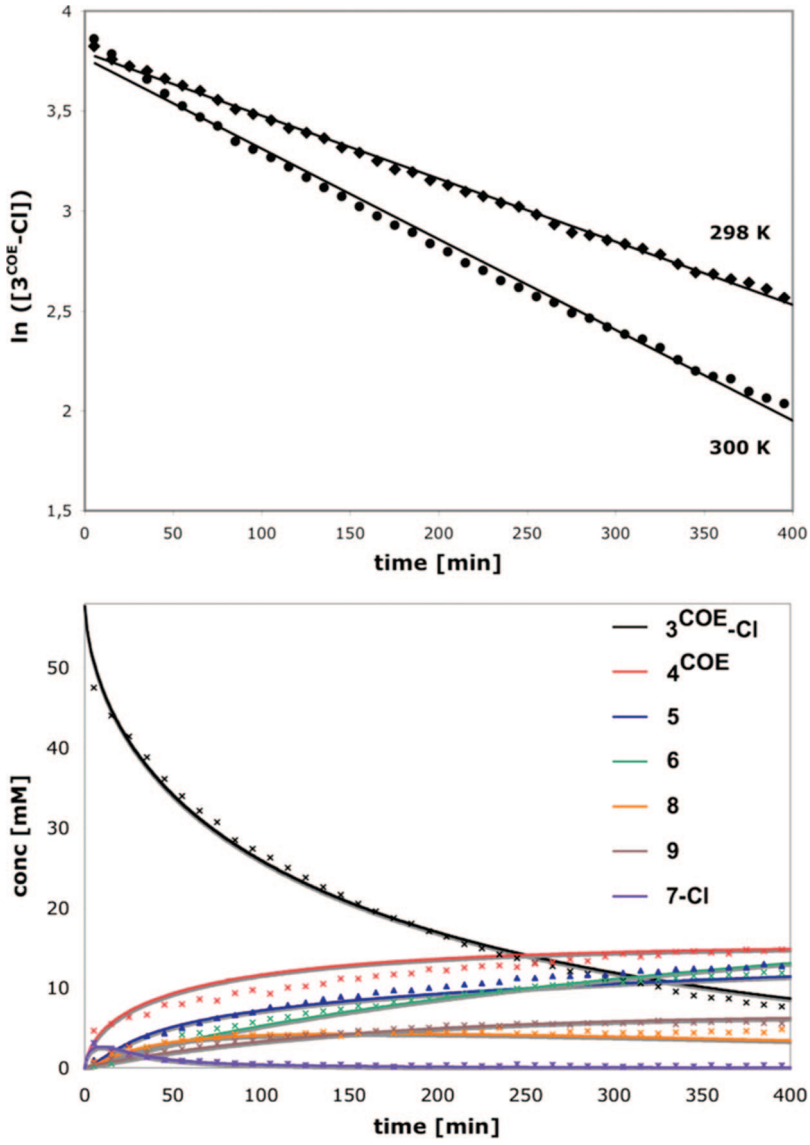

Figure 3. (Top) Decay of $\mathbf{3^{COE}}$**-Cl** in THF at 298 and 300 K. (Bottom) Concentration vs time plot of the reaction of $\mathbf{3^{COE}}$**-PF$_6$** with [N^{n}Bu$_3$(CH$_2$Ph)]Cl in THF at 300 K with experimental (crosses) and fitted (lines) concentrations based on the proposed pathway in Scheme 2.

carbonyl complex [Ir(CO)(PNP)^H]X ($\mathbf{3^{CO}}$**-X**; X = PF_6, BPh_4). Oxidative addition of HCl to $\mathbf{3^{COE}}$**-PF$_6$** affords iridium(III) complex [IrHCl(COE)(PNP)^H]PF_6 (**7-PF$_6$**) in moderate yield.

Clean *N*-deprotonation of $\mathbf{3^L}$**-X** (L = COE, C_2H_4, CO) is obtained by the reaction with KO^{t}Bu in THF, giving rise to [IrL(PNP)] ($\mathbf{4^L}$) (Scheme 4). The highly air-sensitive amido complexes $\mathbf{4^L}$ are very soluble in nonpolar organic solvents such as benzene and pentane.

4. Spectroscopic Characterization. The iridium(I) amino complexes $\mathbf{3^L}$**-PF$_6$** (L = COE, C_2H_4, C_3H_6, CO) exhibit N−H stretching frequencies in the IR spectra between 3223 and 3210 cm^{-1}, which are much closer to that of the free ligand (3285 cm^{-1}) compared with the octahedral iridium(III) complexes [IrH_3(PNP)^H] (3140 cm^{-1}),[17a] **2** (3171 cm^{-1}),[17a] and **5** (3130 cm^{-1}). While N−H···H−Ir hydrogen bonding was proposed for [IrH_3(PNP)^H],[17a] N−H···Cl−Ir hydrogen bonding could account for the low N−H stretching vibration in **2** and **5**. The CO stretching vibration of $\mathbf{3^{CO}}$**-PF$_6$** was observed at 1976 cm^{-1}. Deprotonation of the pincer ligand results in a strong bathochromic shift of this band ($\mathbf{4^{CO}}$: 1908 cm^{-1}), indicating a large increase of electron density at the metal center.

The six-coordinate iridium(III) amino complexes **5**, **6**, and **7-PF$_6$** feature similar solution NMR spectra for the (PNP)^H chelate as **2**.[17a] The singlet in the ^{31}P NMR spectrum, four ^{1}H NMR peaks in the methyl region (doublets of virtual triplets), and two ^{1}H NMR signals assignable to methyne groups indicate a meridional arrangement of the (PNP)^H pincer ligand with two sets of chemically inequivalent isopropyl substituents, each bearing diastereotopic methyl groups, respectively. Accordingly, four signals can be assigned to the ethylene backbone protons, which appear as complex multiplets owing to the complex ABCDXX′ spin system. The hydride chemical shifts of **5** (−24.73 ppm) and **6** (−24.40 ppm) suggest a *trans* arrangement to a chloride ligand, and that of **7-PF$_6$** (−17.83 ppm) indicates a location *trans* to the olefin, as a result of HCl *cis* oxidative addition to $\mathbf{3^{COE}}$**-PF$_6$**.[21] The NMR signals for the cyclooctenyl ligand of **6** are in agreement with vinylic C−H activation featuring the vinylic proton at 6.06 ppm and the olefinic carbon atoms at 124.0 and 134.7 ppm, respectively.

(21) (a) Blake, D. M.; Kubota, M. *Inorg. Chem.* **1970**, *9*, 989. (b) Johnson, C. E.; Eisenberg, R. *J. Am. Chem. Soc.* **1985**, *107*, 6531.

Scheme 3. Syntheses of Iridium PNP Amino Complexes (MX = $AgPF_6$, $NaBPh_4$; L = C_2H_4, C_3H_6)

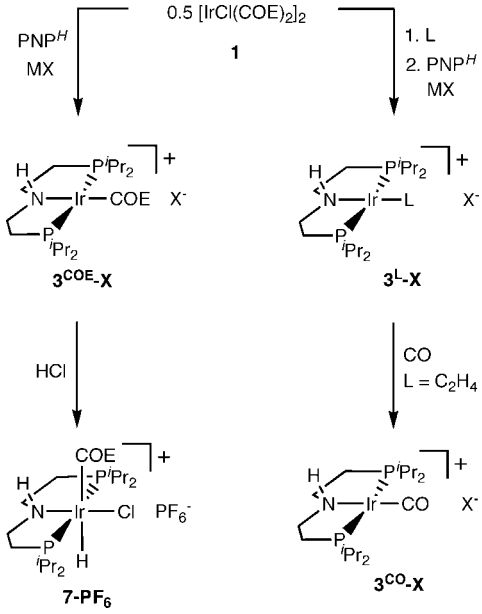

Scheme 4. Synthesis of Iridium PNP Amido Complexes (X = PF_6, BPh_4; L = COE, C_2H_4, CO)

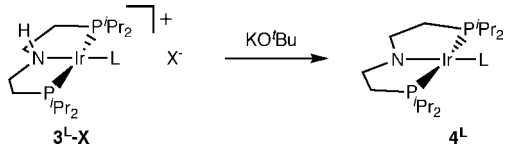

Solution NMR spectra of iridium(I) amino complexes **3^{C2H4}-PF_6**, **3^{COE}-PF_6**, and **3^{CO}-PF_6** resemble those of iridium(III) complexes **5**, **6**, and **7-PF_6** with respect to the number and coupling pattern of the $(PNP)^H$ ligand signals, suggesting C_s symmetry on the NMR time scale. In contrast to this, propylene complex **3^{C3H6}-PF_6** features two sharp doublets in the ^{31}P NMR spectrum with a typical *trans* $^2J_{PP}$ coupling constant (307 Hz). Furthermore, ^1H and ^{13}C signals for the $(PNP)^H$ ligand are in agreement with the absence of the virtual plane, indicating hindered propylene rotation for **3^{C3H6}-PF_6**. This interpretation is further backed by a ^1H-ROESY spectrum, where the doublet signal for the propylene methyl group (1.51 ppm) exhibits strong cross-peaks only with two of the eight chemically inequivalent pincer methyl groups (Figure 4).

The mirror symmetry found for **3^{COE}-PF_6** at room temperature indicates fluxional behavior at room temperature on the NMR time scale. Addition of 0.5 equiv of COE to a solution of **3^{COE}-PF_6** in d_8-THF at room temperature does not result in broadening of the free (5.63 ppm) or bound (3.54 ppm) olefin ^1H NMR signals, respectively. Furthermore, a ^1H-EXSY NMR spectrum at room temperature does not indicate slow olefin exchange (Supporting Information).[22] As in **3^{C2H4}-PF_6**, four sharp peaks for the **3^{COE}-PF_6** backbone ethylene bridges suggest high barriers for inversion of the pyramidal amine nitrogen atom. However, the effect of amine inversion can be demonstrated by fast N−H proton exchange: Addition of 1 equiv of *p*-methylphenol to the corresponding amido complex **4^{COE}** (*vide infra*) results in C_{2v} symmetry on the NMR time scale owing to fast O−H/N−H proton exchange. Cooling to −60 °C slows the equilibrium and the signals for **3^{COE}-OC_7H_7** and **4^{COE}** are observed. While

(22) Perrin, C. L.; Dwyer, T. J. *Chem. Rev.* **1990**, *90*, 935.

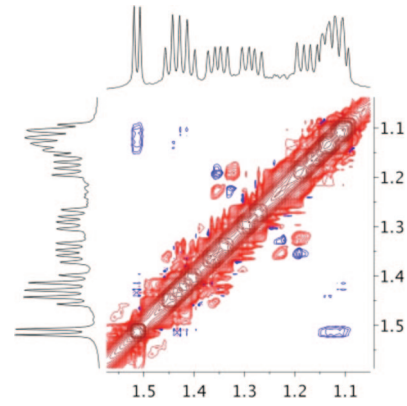

Figure 4. Methyl region of the ^1H-ROESY NMR spectrum of **3^{C3H6}-PF_6**.

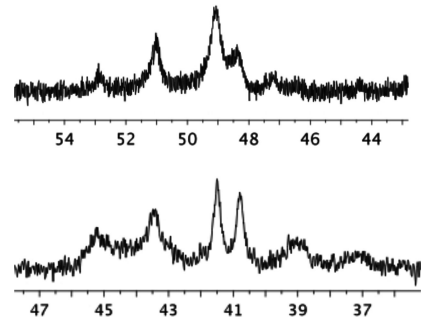

Figure 5. (Top) ^{31}P NMR spectrum of **3^{C3H6}-PF_6** in d_6-acetone at 183 K. (Bottom) ^{31}P NMR spectrum of **3^{COE}-PF_6** in d_8-THF at 173 K.

nitrogen inversion was not observed for **3^{COE}-PF_6**, the ^{15}N chemical shift (δ = −318.8 ppm, $^1H-^{15}N$ HSQC) in d_8-THF shows a small coordination shift relative to the free ligand (δ = −331.2 ppm, $^1H-^{15}N$ HMBC),[23] indicating weak nitrogen coordination to the metal.[24] Furthermore, the **3^{COE}-PF_6** $^1J_{H-N}$ coupling constant (−72 Hz) suggests the absence of strong M···H−N interactions.[25,26]

To further elucidate the fluxional behavior of **3^{COE}-PF_6**, the amino olefin complexes were studied by VT NMR. Cooling of a **3^{C2H4}-PF_6** solution in d_6-acetone to −90 °C does not result in broadening of the ^{31}P and ^1H NMR peaks. However, propylene complex **3^{C3H6}-PF_6** exhibits successive broadening of the two ^{31}P NMR doublets with coalescence of the downfield signal at around −80 °C (Figure 5, Supporting Information). Low-temperature ^{31}P NMR of **3^{COE}-PF_6** in d_6-acetone reveals that the sharp room-temperature signal splits at around −65 °C into two broad peaks, as would be expected for freezing olefin rotation (Supporting Information). However, cooling below −90 °C in d_8-THF results in further splitting of the ^{31}P NMR signals, resulting in a complex pattern of broad peaks at −100 °C, similar to **3^{C3H6}-PF_6** (Figure 5). Between +25 and −100 °C, no peaks assignable to hydrides were found by ^1H NMR

(23) No signal was found in the $^1H-^{15}N$ HSQC NMR spectrum of $(PNP)^H$, presumably due to rapid N−H exchange on the NMR time scale.
(24) Mason, J. *Chem. Rev.* **1981**, *81*, 205.
(25) The $^1J_{HN}$ coupling constant of $HNMe_2$ was reported to be −67 Hz: Alei M., Jr.; Florin, A. E.; Litchman, W. M.; O'Brien, J. F. *J. Phys. Chem.* **1971**, *75*, 932.
(26) (a) Pregosin, P. S.; Rüegger, H.; Wombacher, F.; van Koten, G.; Grove, D. M.; Wehman-Ooyevaar, I. C. M. *Magn. Reson. Chem.* **1992**, *30*, 548. (b) Lee, J. C., Jr.; Müller, B.; Pregosin, P.; Yap, G. P. A.; Rheingold, A. L.; Crabtree, R. H. *Inorg. Chem.* **1995**, *34*, 6295. (c) Yao, W.; Eisenstein, O.; Crabtree, R. H. *Inorg. Chim. Acta* **1997**, *254*, 105.

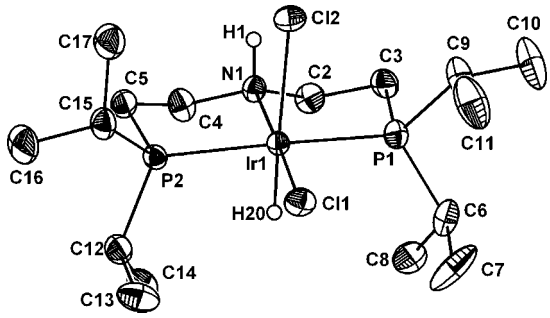

Figure 6. DIAMOND plot of **5** in the crystal (one of the two independent molecules) with thermal ellipsoids drawn at the 50% probability level. Hydrogen atoms other than H1 and H20 are omitted for clarity.

Table 1. Selected Bond Lengths and Angles of 2^{17a} and 5 (corresponding values for the second crystallographically independent molecule in parentheses) in the Crystal

	5		$\mathbf{2}^{17a}$
	Bond Lengths (Å)		
Ir1−H20	1.41(7) (1.30(7))	Ir1−$H1_{Ir}$[a]	1.36(5)
Ir1−Cl1	2.386(1) (2.385(1))	Ir1−$H2_{Ir}$[a]	1.63(5)
Ir1−Cl2	2.524(2) (2.521(1))	Ir1−Cl1	2.506(1)
Ir1−N1	2.091(4) (2.082(4))	Ir1−N1	2.187(3)
Ir1−P1	2.296(2) (2.291(2))	Ir1−P1	2.276(1)
Ir1−P2	2.293(2) (2.298(2))	Ir1−P2	2.276(1)
H1···Cl2	2.70 (2.63)	$H1_N$···Cl1[a]	2.58(7)
	Bond Angles (deg)		
Cl2−Ir1−N1	85.6(1) (84.1(1))	Cl1−Ir−N1	86.8(1)
Cl1−Ir1−Cl2	92.71(5) (94.40(5))	Cl1−Ir−$H2_{Ir}$[a]	91(2)
N1−Ir1−Cl1	176.9(1) (178.5(1))	N1−Ir1−$H2_{Ir}$[a]	178(2)
P1−Ir1−P2	165.81(5) (167.22(5))	P2−Ir1−P2	167.19(4)

[a] $H1_{Ir}$: hydride *trans* to Cl1; $H2_{Ir}$: hydride *trans* to N1; $H1_N$: N−H.

spectroscopy, but all ^{1}H NMR peaks exhibit very strong broadening with half-widths at −100 °C of up to 40 Hz. Furthermore, the sharp ^{31}P and ^{19}F NMR signals of the **3^{COE}-PF_6** counteranion remain unchanged down to −100 °C.

NMR spectra of ethylene amido complexes **4^{C2H4}** and **4^{CO}** are in agreement with C_{2v} symmetry, implying planarization of the dialkylamido backbone on the NMR time scale. On the other hand, NMR spectra of **4^{COE}** indicate the loss of the mirror plane defined by N, Ir, and the olefinic carbon atoms, resulting in two sharp ^{31}P NMR doublets with a $^2J_{PP}$ *trans* coupling constant of 373 Hz. No peak broadening of these signals was observed upon heating to 100 °C in d_8-toluene.

5. X-ray Crystal Structure Determinations. 3^{C2H4}-PF_6, 3^{CO}-PF_6, 4^{C2H4}, 4^{CO}, and **5** were characterized by single-crystal X-ray diffraction. Repeated crystallization attempts for **3^{COE}-PF_6** and **3^{COE}-BPh_4** resulted in heavily disordered crystals. However, the constitution and conformation of the $(PNP)^H$ backbone in the **3^{COE}-BPh_4** cation were confirmed to be analogous to **3^{C2H4}-PF_6** and **3^{CO}-PF_6** (Supporting Information).

The molecular structure of complex **5** (Figure 6, Table 1) in the solid state strongly resembles that of dihydrido chloro compound **2**, which was reported by Clarke et al.[17a] As a major difference, the Ir−N1 bond is considerably shorter in **5** (ΔD_{Ir-N} = 0.1 Å), owing to the weaker *trans*-influence of chloride compared with a hydride ligand. The metal center in **5** is located in a slightly distorted octahedral coordination geometry with a $(PNP)^H$ chelate bite angle of 165.81(5)°. Further distortion arises from bending of Cl2 toward amine proton H1 (Cl2−Ir1−N1: 85.6(1)°) indicative of H1···Cl2 hydrogen bonding (H1···Cl2: 2.70 Å), which is in agreement with IR spectroscopic results.

For iridium(I) amino complexes **3^{L}-PF_6** (L = C_2H_4, CO) the structural assignments in solution are in agreement with the

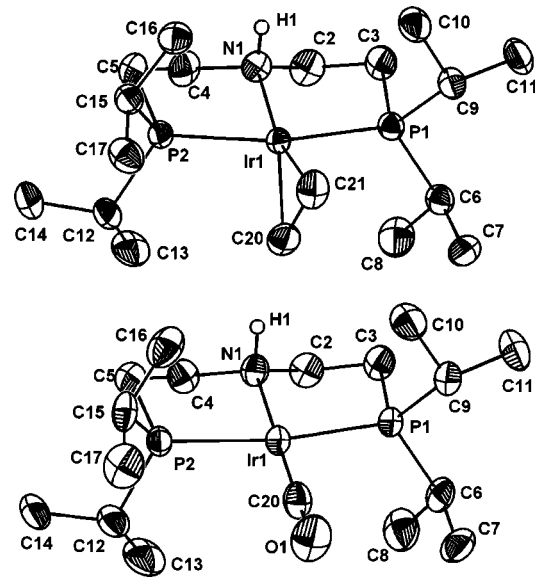

Figure 7. DIAMOND plot of the **3^{C2H4}-PF_6** (above) and **3^{CO}-PF_6** (below) cations in the crystal, respectively, with thermal ellipsoids drawn at the 50% probability level. Calculated hydrogen atoms are omitted for clarity.

Table 2. Selected Bond Lengths and Angles of 3^{C2H4}-PF_6, 3^{CO}-PF_6, 4^{C2H4}, and 4^{CO} (corresponding values for the second crystallographically independent molecule in parentheses) in the Crystal

	3^{C2H4}-PF_6	**3^{CO}-PF_6**	**4^{C2H4}**	**4^{CO}**
		Bond Lengths (Å)		
Ir1−N1	2.131(4)	2.121(6)	1.99(2)	2.035(4) (2.028(4))
Ir1−P1	2.304(1)	2.297(2)	2.277(5)	2.284(1) (2.287(1))
Ir1−P2	2.303(1)	2.300(2)	2.264(5)	2.281(1) (2.293(1))
Ir1−C20	2.145(6)	1.804(7)	2.10(2)	1.839(7) (1.818(6))
Ir1−C21	2.144(6)		2.17(2)	
C20−C21	1.355(9)		1.42(3)	
		Bond Angles (deg)		
P1−Ir1−P2	166.63(4)	166.75(6)	165.49(18)	165.89(5) (164.06(5))
N1−Ir1−C20	159.5(2)	179.8(3)	158.8(8)	177.0(2) (177.9(3))
N1−Ir1−C21	163.7(2)		162.4(7)	
Ir1−C20−O1		178.6(7)		179.3(4) (178.4(4))
Ir1−N1−C2	113.4(3)	113.7(4)	122.4(12)	121.0(3) (122.6(3))
Ir1−N1−C4	114.6(3)	114.7(4)	124.8(13)	122.8(4) (122.5(4))
C2−N1−C4	111.3(4)	109.9(6)	109.5(15)	112.4(4) (110.0(4))

molecular structure in the solid state (Figure 7, Table 2). The cations feature distorted square-planar coordinated iridium centers with $(PNP)^H$ bite angles of 166.63(4)° (**3^{C2H4}-PF_6**) and 166.75(6)° (**3^{CO}-PF_6**), respectively. The Ir1−H1 distances (**3^{C2H4}-PF_6**: 2.47(6) Å; **3^{CO}-PF_6**: 2.54 Å) and Ir1−N−H1 angles (**3^{C2H4}-PF_6**: 104(4)°; **3^{CO}-PF_6**: 106°) are not indicative of an intramolecular M···H−N interaction. The large Ir1−N1 distances (**3^{C2H4}-PF_6**: 2.131(4) Å; **3^{CO}-PF_6**: 2.121(6) Å) are in agreement with strong ethylene and CO *trans*-influences and weak coordinative N→M bonding. The olefinic C═C bond length in **3^{C2H4}-PF_6** (C20−C21: 1.355(9) Å) is very close to the equilibrium C═C distance experimentally found for free ethylene (1.334 Å).[27]

The molecular structures of amido complexes **4^{C2H4}** and **4^{CO}** in the solid state (Figure 8, Table 2) confirm planarization of the amido nitrogen atom (sum of the bond angles around N1: 357° (**4^{C2H4}**), 356° (**4^{CO}**)). Furthermore, covalent amido bonding results in significantly shorter Ir1−N1 bonds (**4^{C2H4}**: 1.99(2) Å; **4^{CO}**: 2.035(4) Å) as compared with the corresponding amino

(27) Duncan, J. L. *Mol. Phys.* **1974**, *28*, 1177.

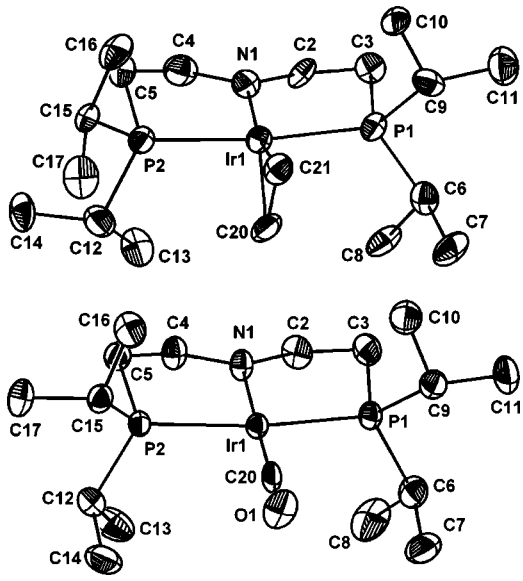

Figure 8. DIAMOND plot of $\mathbf{4^{C2H4}}$ (above) and $\mathbf{4^{CO}}$ (below; one of the two independent molecules) in the crystal, respectively, with thermal ellipsoids drawn at the 50% probability level. Hydrogen atoms are omitted for clarity.

complexes. Most other bond lengths and angles around the metal centers in $\mathbf{4^{C2H4}}$ and $\mathbf{4^{CO}}$ are close to those found in the respective amino complexes, indicating structural flexibility of the ethylene-bridged pincer ligand. The C=C distance in $\mathbf{4^{C2H4}}$ is considerably longer compared with $\mathbf{3^{C2H4}}$-$\mathbf{PF_6}$ ($\Delta D_{C=C} = 0.07$ Å), pointing toward strong M→olefin back-bonding in the amido complex. Accordingly, the angle ϕ of the plane defined by the metal and the ethylene carbon atoms (Ir1, C20, and C21) with the square-planar coordination polyhedron (Ir1, P1, and N1) is closer to ideal 90° ($\mathbf{3^{C2H4}}$-$\mathbf{PF_6}$: 72.3(4)°; $\mathbf{4^{C2H4}}$: 82.7(14)°). Unfortunately, the quality of the $\mathbf{4^{C2H4}}$ crystal structure does not permit localization of the olefinic protons on the electron density map to compare pyramidalization of C20/C21 as a diagnostic tool for their hybridization.

Discussion

1. Reactivity and Fluxional Behavior of $\mathbf{3^{COE}}$-$\mathbf{PF_6}$. Scheme 2 shows our proposed model for the formation of $\mathbf{4^{COE}}$, **5**, and **6** from $\mathbf{3^{COE}}$-**Cl** in nonprotic solvents. The reaction scheme can be broken down in two principle pathways: (1) C−H activation of the COE ligand and trapping by nucleophilic attack of the chloride at the iridium center; (2) chloride base assisted N−H activation and intermolecular HCl oxidative addition. This model explains the observed solvent dependence, as efficient solvation of the chloride ion via hydrogen bonding with protic solvents both increases the barrier to nucleophilic attack and reduces its basicity.[28] It should be pointed out that we have no indication for intramolecular N−H activation, contrasting with other PEP (E = N, C) pincer ligands, such as $HN(RC_6H_3PR_2)_2$, $CH_2(C_2H_4PR_2)_2$, or $C_6H_4(m\text{-}CH_2PR_2)_2$, where E−H oxidative addition is typically observed with Ir^I precursors.[14a,29,30] Given the complexity of the proposed model, it is interesting that a first-order rate was observed for $\mathbf{3^{COE}}$-**Cl**. The rate law for $\mathbf{3^{COE}}$-**Cl**, according to the model, is given by

$$r(\mathbf{3^{COE}}\text{-Cl}) = -k_1[\mathbf{3^{COE}}\text{-Cl}] - k_2[\mathbf{3^{COE}}\text{-Cl}] - k_3[\mathbf{3^{COE}}\text{-Cl}] + k_{-3}[\mathrm{HCl}][\mathbf{4^{COE}}] - k_4[\mathrm{HCl}][\mathbf{3^{COE}}\text{-Cl}] \quad (1)$$

This rate becomes pseudo first order assuming steady-state conditions for c_{HCl}, which is reasonable, as both oxidative addition of HCl to iridium(I) (k_4) and protonation of amido complex $\mathbf{4^{COE}}$ (k_{-3}) should be fast with respect to N−H deprotonation (k_3) as was found in the simulation, as well. Accordingly, calculated c_{HCl} is very small, remaining below 7×10^{-4} M throughout the course of the reaction. Hence, k_{obs} for the decay of $\mathbf{3^{COE}}$-**Cl** (4.5×10^{-3} min^{-1} at 300 K) marks an upper limit for the rates of the formation of C−H activation products **6** and **8**, with calculated values for k_1 and k_2 of 1.4×10^{-3} and 1.0×10^{-3} min^{-1}, respectively. It is unlikely for C−H activation and trapping of the vinyl hydride by Cl^- to proceed concerted, and intermediates such as a five-coordinate hydrido vinyl species are most reasonable. However, the absence of COE exchange for $\mathbf{3^{COE}}$-$\mathbf{PF_6}$ suggests that three-coordinate $[Ir(P\text{-}NP)^H]^+$ is not involved.

Iridium vinyl hydrides have been reported for several stoichiometric and catalytic alkene functionalization reactions, such as alkane dehydrogenation,[31] olefin dimerization,[32] or catalytic vinylic H/D exchange.[33] As usually the η^2-olefin complexes are the thermodynamically favored isomers, they cannot be direct intermediates for thermal vinylic C−H activation in these cases, and separate transition states must account for π-complexation and C−H oxidative addition during the interaction of the metal with an incoming olefin.[34] Stable vinyl hydrides were typically obtained with sterically encumbered auxiliary ligands and alkenes or by trapping of five-coordinate vinyl hydrides with a sixth ligand.[2,31,35] For cyclooctene, iridium complexes resulting from both vinylic[35c,36] and allylic[37] C−H activation are known. In a system related to ours, Milstein reported that the reaction of **1** with the pyridine-based pincer ligand (PNP*) gave hydrido vinyl complex $[IrHCl(C_8H_{13})(PNP^*)]$.[35c]

(28) (a) Regan, C. K.; Craig, S. L.; Brauman, J. I. *Science* **2002**, *296*, 2245. (b) Vayner, G.; Houk, K. N.; Jorgensen, W. L.; Brauman, J. I. *J. Am. Chem. Soc.* **2004**, *126*, 9054. (c) Bordwell, F. G. *Acc. Chem. Res.* **1988**, *21*, 456.

(29) Crocker, C.; Empsall, H. D.; Errington, R. J.; Hyde, E. M.; McDonald, W. S.; Markham, R.; Norton, M. C.; Shaw, B. L.; Weeks, B. *J. Chem. Soc., Dalton Trans.* **1982**, 1217.

(30) (a) Gupta, M.; Hagen, C.; Flesher, R. J.; Kaska, W. C.; Jensen, C. M. *Chem. Commun.* **1996**, 2083. (b) Goldman, A. S.; Ghosh, R. In *Handbook of C-H Transformations - Applications in Organic Synthesis*; Dyker, G., Ed.; Wiley-VCH: New York, 2005; pp 616−621.

(31) Kanzelberger, M.; Singh, B.; Czerw, M.; Krogh-Jespersen, K.; Goldman, A. S. *J. Am. Chem. Soc.* **2000**, *122*, 11017.

(32) Alvarado, Y.; Boutry, O.; Gutierrez, E.; Monge, A.; Nicasio, M. C.; Poveda, M. L.; Perez, P. J.; Ruiz, C.; Bianchini, C.; Carmona, E. *Chem.−Eur. J.* **1997**, *3*, 860.

(33) Torres, F.; Sola, E.; Martin, M.; Lopez, J. A.; Lahoz, F. J.; Oro, L. A. *J. Am. Chem. Soc.* **1999**, *121*, 10632.

(34) (a) Stoutland, P. O.; Bergman, R. G. *J. Am. Chem. Soc.* **1985**, *107*, 4581. (b) Stoutland, P. O.; Bergman, R. G. *J. Am. Chem. Soc.* **1988**, *110*, 5732. (c) Bell, T. W.; addleton, D. M.; McCamley, A.; Partridge, M. G.; Perutz, R. N.; Willner, H. *J. Am. Chem. Soc.* **1990**, *112*, 9212. (d) Bianchini, C.; Barbaro, P.; Meli, A.; Peruzzini, M.; Vacca, A.; Vizza, F. *Organometallics* **1993**, *12*, 2505. (e) Bell, T. W.; Brough, S.-A.; Partridge, M. G.; Perutz, R. N.; Rooney, A. D. *Organometallics* **1993**, *12*, 2933. (f) Smith, K. M.; Poli, R.; Harvey, J. N. *Chem.−Eur. J.* **2001**, *7*, 1679.

(35) Examples: (a) Werner, H.; Dirnberger, T.; Schulz, M. *Angew. Chem.* **1988**, *100*, 993; *Angew. Chem., Int. Ed. Engl.* **1988**, *27*, 948. (b) Ghosh, C. K.; Hoyano, J. K.; Krentz, R.; Graham, W. A. G. *J. Am. Chem. Soc.* **1989**, *111*, 5480. (c) Hermann, D.; Gandelman, M.; Rozenberg, H.; Shimon, L. J. W.; Milstein, D. *Organometallics* **2002**, *21*, 812.

(36) (a) Fernandez, M. J.; Rodriguez, M. J.; Oro, L. A.; Lahoz, F. J. *J. Chem. Soc., Dalton Trans.* **1989**, 2073. (b) Iimura, M.; Evans, D. R.; Flood, T. C. *Organometallics* **2003**, *22*, 5370.

(37) (a) Tanke, R. S.; Crabtree, R. H. *Inorg. Chem.* **1989**, *28*, 3444. (b) Peters, J. C.; Feldman, J. D.; Tilley, T. D. *J. Am. Chem. Soc.* **1999**, *121*, 9871. (c) Budzelaar, P. H. M.; Moonen, N. N. P.; de Gelder, R.; Smits, J. M. M. *Eur. J. Inorg. Chem.* **2000**, 753. (d) Ortmann, D. A.; Gevert, O.; Laubender, M.; Werner, H. *Organometallics* **2001**, *20*, 1776. (e) Turculet, L.; Feldman, J. D.; Tilley, T. D. *Organometallics* **2004**, *23*, 2488.

Table 3. CO Stretching Vibrations of *trans*-Diphosphine Carbonyl Iridium(I) Complexes

complex	ν_{CO} [cm^{-1}]	ref
[Ir(CO){HN(CH$_2$CH$_2$PiPr$_2$)$_2$}]PF$_6$	1976	this work
[Ir(CO){C$_5$H$_3$N(CH$_2$P^{t}Bu$_2$)$_2$}]PF$_6$	1962	40
[Ir(CO){C$_6$H$_3$(OP^{i}Bu$_2$)$_2$}]	1949	41
[Ir(CO)Cl(P^{i}Pr$_3$)$_2$]	1935	42
[Ir(CO){N(SiMe$_2$CH$_2$P^{i}Pr$_2$)$_2$}]	1930	12e
[Ir(CO){N(C$_6$MeH$_3$P^{i}Pr$_2$)$_2$}]	1930	43
[Ir(CO){C$_6$H$_3$(CH$_2$P^{i}Pr$_2$)$_2$}]	1920	44
[Ir(CO){N(CH$_2$CH$_2$P^{i}Pr$_2$)$_2$}]	1908	this work

We hoped for the fluxional behavior of **3^{COE}-PF$_6$** to provide further information. NMR spectroscopic characterization suggests rigid olefin binding for **3^{C3H6}-PF$_6$**. Furthermore, the molecular structure of **3^{C2H4}-PF$_6$** in the crystal features the olefin embedded in the cavity formed by the ^{i}Pr substituents with several close contacts to the pincer ligand. Therefore, for sterically more stressed **3^{COE}-PF$_6$** rapid olefin rotation seems unlikely as the origin of the fluxional behavior.[38] Olefin exchange, anion coordination, and amine inversion can further be excluded. Unfortunately, low-temperature NMR of **3^{COE}-PF$_6$** remains inconclusive. However, a similarly complex pattern in the ^{31}P NMR and very broad ^{1}H NMR peaks were found for the (PNP)^H ligand signals of **3^{C3H6}-PF$_6$**, which is not fluxional at room temperature with respect to the olefin moiety. On the basis of the observed reactivity of **3^{COE}-Cl**, we suggest that the fluxionality of **3^{COE}-PF$_6$** can be explained with rapid, reversible vinylic C−H activation of the COE ligand. The lack of observable hydride signals in the ^{1}H NMR at any temperatures indicates that the equilibrium must be shifted toward the olefin complex. However, further dynamic processes, e.g., isopropyl rotation or hemilability of the nitrogen donor, seem to be freezing in the same temperature range, so that quantitative kinetic data could not be extracted.

2. Comparison of Amino and Amido Complexes. In contrast to **3^{COE}-PF$_6$**, amido complex **4^{COE}** features rigid olefin binding up to 100 °C on the NMR time scale. Since sterics should be comparable in these complexes, electronic factors must mainly account for the different behavior. The CO stretching vibrations of **3^{COE}-PF$_6$** and **4^{CO}** are at the far ends of a range of iridium(I) diphosphine carbonyl complexes (Table 3), suggesting a substantial increase in electron density at the metal center upon deprotonation of the (PNP)^H nitrogen. Further indication is provided by the large increase in olefinic C=C bond distance upon N-deprotonation of the ethylene amino complex (**3^{C2H4}-PF$_6$/4^{C2H4}**: $\Delta D_{C=C} = 0.07$ Å). Almost identical olefinic ^{13}C upfield shifts (**3^{C2H4}-PF$_6$/4^{C2H4}**: $\Delta\delta_{13C} = 22.1$ ppm; **3^{COE}-PF$_6$/4^{COE}**: $\Delta\delta_{13C} = 20.8$ ppm) suggest comparable effects on COE binding.[39]

Therefore, we attribute the structural rigidity of **4^{COE}**, as compared with **3^{COE}-PF$_6$**, to strong Ir→COE back-bonding. The electron density at the metal will be strongly enhanced by repulsive π-interaction of the amido lone pair with a filled metal d-orbital, which is involved in Ir→L$_{trans}$ (L = olefin, CO) back-bonding, as well. Although the higher electron density in the amido complexes should make Ir^{III} thermodynamically more accessible, the increase in Ir−olefin binding strength prevents the olefin complexes from rearrangement. The conjugate acid/base pair **3^{COE}-PF$_6$** and **4^{COE}** therefore represents an unprecedented example of metal complexes with switchable vinylic olefin C−H activation by de/protonation of the pincer auxiliary ligand (Scheme 5).

Scheme 5. Proposed Switchable C−H Activation for 3^{COE}-PF$_6$ and 4^{COE}

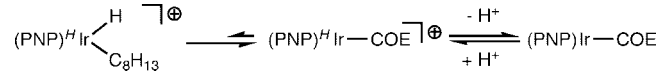

Conclusions

In conclusion, we described the synthesis of a new class of iridium(I) amino and amido complexes bearing the PNP pincer ligand N(CH$_2$CH$_2$P^{i}Pr$_2$)$_2$. The instability of **3^{COE}-Cl** in nonprotic solvents is attributed to both anion-assisted N−H deprotonation and trapping of vinylic C−H activation products. No indications for M···H−N interactions or intramolecular N−H oxidative addition were found. Our results suggest that **3^{COE}-PF$_6$** is a rare example of an olefin complex that exhibits a fast equilibrium with a vinyl hydride isomer at room temperature on the NMR time scale, accounting at least in part for the observed fluxionality. Unfortunately, other dynamic processes on the pincer ligand seem to be coupled, preventing the extraction of quantitative data. On the other hand, the structural rigidity of the corresponding amido complex **4^{COE}** is attributed to strong olefin binding, which is reinforced by the N−Ir−olefin 3c−4e π-interaction and illustrates the electron-rich character of the Ir(PNP) fragment. Using the olefin ligand as a probe for Ir−N bonding, this interpretation renders **3^{COE}-PF$_6$/4^{COE}** an interesting system that features switchable C−H activation upon de/protonation of the pincer ligand.

Experimental Section

Materials and Synthetic Methods. All experiments were carried out under an atmosphere of argon using Schlenk and glovebox techniques. The solvents were dried over Na/benzophenone/tetraglyme (benzene) or Na/benzophenone (THF), distilled under argon, and deoxygenated prior to use. Deuterated solvents were dried by distillation from Na/K alloy (C_6D_6 and d_8-THF), stirring over 4 Å molecular sieves, and distillation from B_2O_3 (d_6-acetone) or distillation from CaH_2 (CD_2Cl_2), respectively, and deoxygenated by three freeze−pump−thaw cycles. KO^{t}Bu and cyclooctene were purchased from VWR and sublimed (KO^{t}Bu)/distilled (cyclooctene) prior to use. Ethene 2.7 (Messer Griesheim), propylene 2.8 (Gerling, Holz + Co.), and iridiumtrichloride hydrate (ABCR) were used as purchased. HN(CH$_2$CH$_2$P^{i}Pr$_2$)$_2$[45] and [IrCl(COE)$_2$]$_2$ (**1**)[46] were prepared as reported in the literature.

Analytical Methods. Elemental analyses were obtained from the Microanalytical Laboratory of Technische Universität München. The IR spectra were recorded on a Jasco FT/IR-460 PLUS

(38) Activation parameters for hypothetical olefin rotation for **3^{COE}-PF$_6$** were estimated by line-shape analysis of the ^{31}P NMR signals to be in the range of $\Delta G^{\ddagger}_{300} \approx 37$ kJ·mol^{-1}.

(39) Although rationalization of metal−olefin bonding on the basis of pure ^{13}C olefin coordination shifts has been discussed controversially, within closely related systems it is justified to use $\Delta\delta_{13C}$ values as a qualitative indicator for relative M→olefin back-bonding: (a) Thoennes, D. J.; Wilkins, C. L.; Trahanovsky, W. S. *J. Magn. Reson.* **1974**, *13*, 18. (b) Evans, J.; Norton, J. R. *Inorg. Chem.* **1974**, *13*, 3042. (c) Clark, P. W.; Hanisch, P.; Jones, A. J. *Inorg. Chem.* **1979**, *18*, 2067.

(40) Kloeck, S. M.; Heinekey, M.; Goldberg, K. I. *Organometallics* **2006**, *25*, 3007.

(41) Göttker-Schnetmann, I.; White, P. S.; Brookhart, M. *Organometallics* **2004**, *23*, 1766.

(42) Faraone, F.; Piraino, P.; Pietropaolo, R. *J. Chem. Soc., Dalton Trans.* **1973**, 1625.

(43) Whithead, M. T.; Grubbs, R. H. *J. Am. Chem. Soc.* **2008**, *130*, 5874.

(44) Rybtchinski, B.; Ben-David, Y.; Milstein, D. *Organometallics* **1997**, *16*, 3786.

(45) Danopoulos, A. A.; Wills, A. R.; Edwards, P. G. *Polyhedron* **1990**, *9*, 2413.

(46) Onderlinden, A. L.; van der Ent, A. *Inorg. Chim. Acta* **1972**, *6*, 420.

Table 4. Crystallographic Data for [Ir(C_2H_4)(PNP)^H][PF_6] (3^{C2H4}-PF_6), [Ir(CO)(PNP)^H][PF_6] (3^{CO}-PF_6), [Ir(C_2H_4)(PNP)] (4^{C2H4}), [Ir(CO)(PNP)] (4^{CO}), and [$IrHCl_2$(PNP)^H] (5)

	3^{C2H4}-PF_6	3^{CO}-PF_6	4^{C2H4}	4^{CO}	5
formula	$C_{18}H_{41}F_6IrNP_3$	$C_{17}H_{37}F_6IrNOP_3$	$C_{18}H_{40}IrNP_2$	$C_{17}H_{36}IrNOP_2$	$C_{16}H_{38}Cl_2IrNP_2$
fw	670.65	670.61	524.67	524.63	569.53
color/habit	red/fragment	yellow/fragment	yellow/plate	yellow/plate	colorless/fragment
cryst dimens (mm^3)	0.18 × 0.20 × 0.25	0.05 × 0.18 × 0.46	0.05 × 0.25 × 0.33	0.02 × 0.25 × 0.25	0.20 × 0.33 × 0.38
cryst syst	monoclinic	monoclinic	triclinic	triclinic	triclinic
space group	$P2_1/c$ (no. 14)	$P2_1/c$ (no. 14)	$P\bar{1}$ (no. 2)	$P\bar{1}$ (no. 2)	$P\bar{1}$ (no. 2)
a, Å	8.7145(4)	8.6581(1)	8.967(2)	7.6119(4)	11.8102(4)
b, Å	15.9371(5)	15.6096(2)	10.632(3)	13.5411(7)	14.2081(5)
c, Å	18.3834(9)	18.5711(2)	12.933(4)	21.8518(12)	14.5239(4)
α, deg	90	90	70.12(2)	78.202(4)	101.423(3)
β, deg	96.488(4)	94.818(1)	83.63(2)	80.638(4)	101.801(3)
γ, deg	90	90	70.30(2)	73.614(4)	106.574(3)
V, Å^3	2536.81(19)	2501.01(5)	1091.6(6)	2102.0(2)	2199.45(14)
Z	4	4	2	4	4
T, K	173	153	193	173	153
D_{calcd}, g cm^{-3}	1.756	1.781	1.596	1.658	1.720
μ, mm^{-1}	5.502	5.583	6.261	6.506	6.457
F(000)	1328	1320	524	1040	1128
θ range, deg	3.98−26.79	2.99−25.30	3.71−22.46	3.90−26.79	2.81−25.38
index ranges (h, k, l)	±11, ±20, ±23	±10, ±18, ±22	±9, ±11, ±13	±9, ±17, ±27	±14, ±17, ±17
no. of rflns collected	34 278	29 964	4107	36 155	39 372
no. of indep rflns/R_{int}	5346/0.069	4554/0.046	2078/0.106	8863/0.073	7989/0.026
no. of obsd rflns ($I > 2\sigma(I)$)	4723	3506	1671	6818	6440
no. of data/restraints/params	5346/0/290	4554/0/270	2078/0/207	8863/0/413	7989/0/421
R1/wR2 ($I > 2\sigma(I)$)[a]	0.0317/ 0.0632	0.0360/0.0893	0.0523/0.1278	0.0301/0.0724	0.0256/0.0506
R1/wR2 (all data)[a]	0.0393/0.0655	0.0535/0.1038	0.0689/0.1350	0.0405/0.0741	0.0445/0.0632
GOF (on F^2)[a]	1.100	1.075	0.988	0.903	1.202
largest diff peak and hole (e Å^{-3})	+1.21/−1.26	+2.78/−1.03	+1.13/−1.08	+1.21/−1.86	+2.77/−1.21

[a] $R1 = \sum(||F_o| - |F_c||)/\sum|F_o|$; $wR2 = \{\sum[w(F_o^2 - F_c^2)^2]/\sum[w(F_o^2)^2]\}^{1/2}$; $GOF = \{\sum[w(F_o^2 - F_c^2)^2]/(n - p)\}^{1/2}$.

spectrometer as Nujol mulls between KBr plates. NMR spectra were recorded on Jeol Lambda 400, Bruker DPX 400, Bruker DMX 500, and Bruker DMX 600 spectrometers at room temperature and were calibrated to the residual proton resonance and the natural abundance ^{13}C resonance of the solvent (C_6D_6, $\delta_H = 7.16$ and $\delta_C = 128.1$ ppm; d_6-acetone, $\delta_H = 2.05$ and $\delta_C = 29.8 + 206.3$ ppm; d_8-THF, $\delta_H = 1.73 + 3.58$ ppm and $\delta_C = 25.4 + 67.6$ ppm). ^{31}P NMR NMR chemical shifts are reported relative to external phosphoric acid (δ 0.0 ppm). ^{15}N NMR shifts are given relative to $MeNO_2$ by referencing with external ^{15}N-urea in d_6-dmso (δ −302.1 ppm). Signal multiplicities are abbreviated as s (singlet), d (doublet), t (triplet), vt (virtual triplet), sp (septet), m (multiplet), br (broad).

Syntheses. [Ir(COE)(PNP)^H][PF_6] (3^{COE}-PF_6). $HN(CH_2CH_2P^iPr_2)_2$ (0.142 g; 0.466 mmol) is added to a solution of **1** (0.200 g; 0.223 mmol) and $AgPF_6$ (0.118 g; 0.466 mmol) in THF (5 mL) and stirred for 30 min. After filtration the orange product is precipitated with pentanes, washed twice with pentanes, and dried *in vacuo*. Yield: 0.229 g (0.377 mmol; 84%). Anal. Calcd for $C_{24}H_{51}F_6IrNP_3$ (752.80): C, 38.29; H, 6.83; N, 1.86. Found: 38.28; H, 7.11; N, 1.91. IR (cm^{-1}): ν = 3215 (N−H). NMR (d_6-acetone, rt, [ppm]) ^1H NMR (399.8 MHz): δ 1.20 (dvt, $^3J_{HH} = 6.7$ Hz, $J_{PH} = 6.7$ Hz, 6H, CH_3), 1.28 (dvt, $^3J_{HH} = 6.7$ Hz, $J_{PH} = 6.7$ Hz, 6H, CH_3), 1.34 (dvt, $^3J_{HH} = 8.6$ Hz, $J_{PH} = 7.3$ Hz, 6H, CH_3), 1.35 (2H, CH_2^{COE}), 1.40 (dvt, $^3J_{HH} = 7.3$ Hz, $J_{PH} = 8.6$ Hz, 6H, CH_3), 1.49 (m, 4H, CH_2^{COE}), 1.64 (m, 4H, CH_2^{COE}), 1.88 (m, 2H, PCH_2), 2.25−2.32 (m, 4H, $PCH_2 + CH_2^{COE}$), 2.41 (spvt, $^3J_{HH} = 7.0$ Hz, $J_{PH} = 2.8$ Hz, 2H, $CH(CH_3)_2$), 2.54 (spvt, $^3J_{HH} = 7.0$ Hz, $J_{PH} = 2.8$ Hz, 2H, $CH(CH_3)_2$), 2.70 (m, 2H, NCH_2), 3.33 (m, 2H, NCH_2), 3.62 (br, 2H, CH^{COE}), 5.35 (br, 1H, N*H*). $^{13}C\{^1H\}$ NMR (100.6 MHz): δ 16.9 (s, CH_3), 18.5 (s, CH_3), 18.9 (s, CH_3), 24.3 (vt, $J_{CP} = 13.8$ Hz, $CH(CH_3)_2$), 24.5 (vt, $J_{CP} = 14.5$ Hz, PCH_2), 25.7 (vt, $J_{CP} = 13.0$ Hz, $CH(CH_3)_2$), 26.3 (s, CH_2^{COE}), 31.6 (s, CH_2^{COE}), 33.8 (s, CH_2^{COE}), 52.3 (s, CH^{COE}), 55.8 (d, $^2J_{CP} = 2$ Hz, NCH_2). ^{31}P $\{^1H\}$ NMR (161.8 MHz): δ 43.1 (s, P^iPr_2), −143.6 (sp, $^1J_{PF} = 707$ Hz, PF_6). Assignments were confirmed by a $^1H-^1H$ COSY spectrum. [Ir(COE)(PNP)^H][BPh_4] ($\mathbf{3^{COE}}$-$\mathbf{BPh_4}$) can be prepared analogously by using $NaBPh_4$ instead of $AgPF_6$ (yield 90%). The cation exhibits identical ^1H, ^{13}C, and ^{31}P NMR spectra to those in $\mathbf{3^{COE}}$-$\mathbf{PF_6}$.

[Ir(C_2H_4)(PNP)^H][PF_6] (3^{C2H4}-PF_6). Ethylene is bubbled through a suspension of **1** (0.402 g, 0.449 mmol) in acetone (10 mL) at −30 °C until a clear colorless solution occurs. Consecutively a solution of $AgPF_6$ (0.215 g, 0.850 mmol) in acetone (5 mL) and a solution of $HN(CH_2CH_2P^iPr_2)_2$ (0.260 g, 0.851 mmol) in acetone (5 mL) are added at −30 °C. The resulting red suspension is warmed to rt and filtered. Precipitation with pentane gives a red oil, which is redissolved in THF, filtered, and precipitated with diethyl ether and pentane. $\mathbf{3^{C2H4}}$-$\mathbf{PF_6}$ is obtained as a red crystalline product upon filtration, washing with diethyl ether, and drying *in vacuo*. Yield: 0.403 g (0.601 mmol; 67%). Anal. Calcd for $C_{18}H_{41}F_6IrNP_3$ (670.65): C, 32.24; H, 6.16; N, 2.09. Found: C, 32.56; H, 5.81; N, 2.07. IR (cm^{-1}): ν = 3210 (N−H). NMR (d_6-acetone, rt, [ppm]) ^1H NMR (399.78 MHz): δ 1.19 (dvt, $^3J_{HH} = 7.2$ Hz, $J_{HP} = 7.2$ Hz, 6H, CH_3), 1.25 (m, 18H, CH_3), 1.95 (m, 2H, PCH_2), 2.35 (m, 2H, PCH_2), 2.45 (m, 2H, $CH(CH_3)_2$), 2.58 (m, 2H, $CH(CH_3)_2$), 2.75 (m, 2H, NCH_2), 2.88 (t, $^3J_{HH} = 4.0$ Hz, 4H, C_2H_4), 3.45 (m, 2H, NCH_2), 5.70 (br, 1H, N*H*). $^{13}C\{^1H\}$ NMR (100.6 MHz): δ 17.8 (s, CH_3), 17.9 (s, CH_3), 18.7 (s, CH_3), 18.9 (s, CH_3), 23.9 (vt, $J_{CP} = 14.6$ Hz, $CH(CH_3)_2$), 25.0 (vt, $J_{CP} = 13.0$ Hz, PCH_2), 25.3 (vt, $J_{CP} = 13.1$ Hz, $CH(CH_3)_2$), 31.9 (s, C_2H_4), 57.1 (s, NCH_2). $^{31}P\{^1H\}$ NMR (161.8 MHz): δ 49.0 (s, P^iPr_2), −143.6 (sp, $^1J_{PF} = 707$ Hz, PF_6). [Ir(C_2H_4)(PNP)^H][BPh_4] ($\mathbf{3^{C2H4}}$-$\mathbf{BPh_4}$) can be prepared analogously by using $NaBPh_4$ instead of $AgPF_6$ (yield 81%). The cation exhibits identical ^1H, ^{13}C, and ^{31}P NMR spectra to those in $\mathbf{3^{C2H4}}$-$\mathbf{PF_6}$.

[Ir(C_3H_6)(PNP)^H][PF_6] (3^{C3H6}-PF_6). **1** (0.200 g, 0.223 mmol) is suspended in THF (10 mL) at −80 °C and propylene bubbled through the solution for 20 min. After addition of $HN(CH_2CH_2P^iPr_2)_2$ (0.136 g, 0.445 mmol) and $AgPF_6$ (0.113 g, 0.446 mmol) the solution is stirred for 1 h at −80 °C. Upon addition of pentane the crude product is precipitated, filtered off, and redissolved in THF. After filtration the product was precipitated as orange microcrystals with pentane, filtered off, and dried *in vacuo*.

Yield: 0.169 g (0.249 mmol; 55%). Anal. Calcd for $C_{19}H_{43}F_6IrNP_3$ (684.68): C, 33.33; H, 6.33; N, 2.05. Found: C, 32.83; H, 6.15; N, 2.02. IR (cm^{-1}): ν = 3220 (N−H). NMR (d_8-THF, rt, [ppm]) ^1H NMR (399.78 MHz): δ 1.09−1.14 (m, 9H, 3 × PCHCH_3), 1.17 (dd, $^3J_{HH}$ = 5.6 Hz, $^3J_{HP}$ = 10.6 Hz, 3H, PCHCH_3), 1.28 (dd, $^3J_{HH}$ = 5.6 Hz, $^3J_{HP}$ = 10.0 Hz, 3H, PCHCH_3), 1.35 (dd, $^3J_{HH}$ = 5.3 Hz, $^3J_{HP}$ = 9.7 Hz, 3H, PCHCH_3), 1.42 (dd, $^3J_{HH}$ = 6.5 Hz, $^3J_{HP}$ = 12.3 Hz, 3H, PCHCH_3), 1.44 (dd, $^3J_{HH}$ = 5.6 Hz, $^3J_{HP}$ = 11.2 Hz, 3H, PCHCH_3), 1.51 (d, $^3J_{HH}$ = 4.7 Hz, 3H, H_2C=CHCH_3), 1.93−2.10 (m, 3H, 3 × PCH_2), 2.22 (m, 2H, 1 × PCH_2 + PCHMe$_2$), 2.38 (dsp, $^3J_{HP}$ = 5.0 Hz, $^3J_{HH}$ = 5.3 Hz, 1H, PCHMe$_2$), 2.47−2.62 (m, 4H, 1 × H_2C=CHMe + 2 × NCH_2 + PCHMe$_2$), 2.71 (dsp, $^3J_{HP}$ = 5.6 Hz, $^3J_{HH}$ = 5.3 Hz, 1H, PCHMe$_2$), 2.95 (dt, $^3J_{HH}$ = 7.9 Hz, $^3J_{HP}$ = 5.3 Hz, 1H, H_2C=CHMe), 3.34 (dm, $^3J_{HP}$ = 29.0 Hz, 1H, 1 × NCH_2), 3.49 (dm, $^3J_{HP}$ = 27.8 Hz, 1H, 1 × NCH_2), 3.72 (m, 1H, H_2C=CHMe), 5.09 (br, 1H, NH). $^{13}C\{^1H\}$ NMR (100.6 MHz): δ 16.7 (s, PCH*C*H$_3$), 16.8 (s, PCH*C*H$_3$), 17.0 (s, PCH*C*H$_3$), 17.2 (s, 2 × PCH*C*H$_3$), 17.4 (s, PCH*C*H$_3$), 18.6 (d, $^2J_{PC}$ = 3.1 Hz, PCH*C*H$_3$), 19.0 (d, $^2J_{PC}$ = 2.3 Hz, PCH*C*H$_3$), 22.5 (s, H_2C=*C*HCH$_3$), 23.7 (d, $^1J_{CP}$ = 20.7 Hz, P*C*H$_2$), 25.2 (dd, $^1J_{CP}$ = 21.4 Hz, $^3J_{CP}$ = 5.7 Hz, *C*H(CH$_3$)$_2$), 26.3 (dd, $^1J_{CP}$ = 21.4 Hz, $^3J_{CP}$ = 4.6 Hz, *C*H(CH$_3$)$_2$), 32.7 (s, H_2*C*=CHCH$_3$), 42.3 (s, H_2C=*C*HCH$_3$), 56.1 (t, $^2J_{PC}$ = 3.8 Hz, N*C*H$_2$), 57.0 (t, $^2J_{PC}$ = 3.1 Hz, N*C*H$_2$). One P*C*H$_2$ and two *C*H(CH$_3$)$_2$ ^{13}C signals are superimposed with one of the solvent signals. $^{31}P\{^1H\}$ NMR (161.8 MHz): δ 50.6 (d, $^2J_{PP}$ = 307 Hz, *P*^{i}Pr$_2$), 47.5 (d, $^2J_{PP}$ = 307 Hz, *P*^{i}Pr$_2$), −143.7 (sp, $^1J_{PF}$ = 711 Hz, *P*F$_6$).

[Ir(CO)(PNP)^H][PF$_6$] (3^{CO}-PF$_6$). CO is bubbled through a solution of **3^{C2H4}-PF$_6$** (0.136 g, 0.203 mmol) in THF (10 mL) at rt until a yellow, clear solution is obtained. After filtration **3^{CO}-PF$_6$** precipitates upon addition of diethyl ether and pentane as a yellow crystalline product, which is filtered off, washed with pentane, and dried *in vacuo*. Yield: 0.130 g (0.194 mmol; 95%). Anal. Calcd for $C_{17}H_{37}F_6IrNOP_3$ (670.61): C, 30.45; H, 5.56; N, 2.09. Found: C, 31.20; H, 5.47; N, 2.05. IR (cm^{-1}): ν = 3223 (N−H), 1976 (s, CO). NMR (C_6D_6, rt, [ppm]) ^1H NMR (399.78 MHz): δ 0.81 (dvt, $^3J_{HH}$ = 7.2 Hz, J_{HP} = 7.2 Hz, 6H, CH_3), 0.87 (dvt, $^3J_{HH}$ = 7.2 Hz, J_{HP} = 7.2 Hz, 12H, CH_3), 0.91 (dvt, $^3J_{HH}$ = 7.2 Hz, J_{HP} = 7.2 Hz, 12H, CH_3), 1.06 (dvt, $^3J_{HH}$ = 7.6 Hz, J_{HP} = 7.2 Hz, 6H, CH$_3$), 1.78 (m, 6H, PCH_2 + NCH_2), 2.09 (m, 4H, CH(CH$_3$)$_2$), 3.46 (m, 2H, NCH_2), 4.79 (br, 1H, NH). $^{13}C\{^1H\}$ NMR (100.6 MHz): δ 18.0 (s, *C*H$_3$), 18.2 (s, *C*H$_3$), 18.9 (s, *C*H$_3$), 19.0 (s, *C*H$_3$), 24.2 (vt, J_{CP} = 12.2 Hz, *C*H(CH$_3$)$_2$), 25.9 (vt, J_{CP} = 16.1 Hz, P*C*H$_2$), 26.6 (vt, J_{CP} = 15.2 Hz, *C*H(CH$_3$)$_2$), 55.6 (s, N*C*H$_2$), 180.8 (t, $^2J_{CP}$ = 8.0 Hz, *C*O). $^{31}P\{^1H\}$ NMR (161.8 MHz): δ 69.8 (s, *P*^{i}Pr$_2$), −142.53 (sp, $^1J_{PF}$ = 712 Hz, *P*F$_6$).

[Ir(COE)(PNP)] (4^{COE}). KO^{t}Bu (0.015 g, 0.133 mmol) is added to a solution of **3^{COE}-[PF$_6$]** (0.100 g, 0.133 mmol) in THF (5 mL) and stirred for 2 h at rt. The solvent is evaporated *in vacuo* and the residue extracted with pentane, filtered, and evaporated *in vacuo* to give an orange-yellow solid. Yield: 0.058 g (0.95 mmol; 72%). Anal. Calcd for $C_{24}H_{50}IrNP_2$ (606.83): C, 47.50; H, 8.31; N, 2.31. Found: 47.03; H, 8.42; N, 2.28. NMR (C_6D_6, rt, [ppm]) ^1H NMR (399.78 MHz): δ 1.03 (m, 12H, 4 × CH_3), 1.19 (dd, $^3J_{HH}$ = 7.6 Hz, $^3J_{HP}$ = 12.8 Hz, 6H, 2 × CH_3), 1.31 (dd, $^3J_{HH}$ = 7.2 Hz, $^3J_{HP}$ = 12.8 Hz, 6H, 2 × CH_3), 1.42 (m, 2H, CH=CHCH_2), 1.59 (m, 6H, PCH_2 + CH_2^{COE}), 1.73 (dt, $^2J_{HP}$ = 7.2 Hz,$^3J_{HH}$ = 6.8 Hz, 2H, PCH_2), 1.82 (m, 2H, CH_2^{COE}) 1.97 (m, 6H, 4 × CH(CH$_3$)$_2$ + CH_2^{COE}), 2.40 (m, 4H, CH=CHCH_2 + HC=CH), 3.32 (dt, $^3J_{HP}$ = 14.6 Hz,$^3J_{HH}$ = 6.7 Hz, 2H, NCH_2), 3.43 (dt, $^3J_{HP}$ = 16.5 Hz,$^3J_{HH}$ = 6.1 Hz, 2H, NCH_2). $^{13}C\{^1H\}$ NMR (100.6 MHz): δ 17.7 (s, *C*H$_3$), 17.9 (s, *C*H$_3$), 19.2 (d, $^2J_{CP}$ = 2.3 Hz, *C*H$_3$), 20.2 (d, $^2J_{CP}$ = 4.5 Hz, *C*H$_3$), 23.5 (dd, $^1J_{CP}$ = 20.7 Hz,$^3J_{CP}$ = 5.4 Hz, *C*H(CH$_3$)$_2$), 25.8 (dd, $^1J_{CP}$ = 17.0 Hz,$^3J_{CP}$ = 7.0 Hz, *C*H(CH$_3$)$_2$), 26.1 (dd, $^1J_{CP}$ = 24.0 Hz, $^3J_{CP}$ = 3.1 Hz, P*C*H$_2$), 27.5 (s, *C*H$_2^{COE}$), 28.9 (d, $^1J_{CP}$ = 22.1 Hz, P*C*H$_2$), 31.5 (s, HC=*C*H), 33.7 (s, *C*H$_2^{COE}$), 35.3 (m, CH=CH*C*H$_2$), 63.6 (dd, $^2J_{CP}$ = 3.8 Hz,$^4J_{CP}$ = 2.3 Hz, N*C*H$_2$), 64.6 (dd, $^2J_{CP}$ = 5.3 Hz, $^4J_{CP}$ = 3.8 Hz, N*C*H$_2$). $^{31}P\{^1H\}$ NMR (161.8 MHz): δ 49.9 (d, $^2J_{PP}$ = 373 Hz, *P*^{i}Pr$_2$), 53.6 (d, $^2J_{PP}$ = 373 Hz, *P*^{i}Pr$_2$). Assignments were confirmed by $^1H-^1H$ COSY and $^1H-^{13}C$ HETCOR spectra.

[Ir(C$_2$H$_4$)(PNP)] (4^{C2H4}). KO^{t}Bu (0.011 g; 0.096 mmol) in THF (5 mL) is added to a solution of **3^{C2H4}-BPh$_4$** (0.081 g; 0.096 mmol) in 5 mL of THF at 0 °C. The yellow solution is stirred for 1 h, and the solvent evaporated and extracted with pentanes. Evaporation of the solvent gives **4^{C2H4}** as a yellow, microcrystalline solid. Yield: 0.036 g (0.069 mmol; 72%). Anal. Calcd for $C_{18}H_{40}IrNP_2$ (524.68): C, 41.20; H, 7.68; N, 2.68. Found: C, 40.80; H, 7.16; N 2.66. NMR (C_6D_6, rt, [ppm]) ^1H NMR (399.78 MHz): δ 1.04 (dvt, $^3J_{HH}$ = 7.2 Hz, J_{HP} = 7.2 Hz, 12H, CH_3), 1.16 (dvt, $^3J_{HH}$ = 7.2 Hz, J_{HP} = 7.2 Hz, 12H, CH_3), 1.34 (m, 4H, PCH_2), 1.64 (m, 2H, CH(CH$_3$)$_2$), 1.91 (t, $^3J_{HH}$ = 4.4 Hz, 4H, C$_2H_4$), 1.92 (m, 2H, CH(CH$_3$)$_2$), 3.40 (m, 4H, NCH_2). $^{13}C\{^1H\}$ NMR (100.6 MHz): δ 9.8 (s, *C*$_2$H$_4$), 17.7 (s, *C*H$_3$), 19.0 (s, *C*H$_3$), 23.9 (vt, J_{CP} = 13.0 Hz, *C*H(CH$_3$)$_2$), 26.9 (vt, J_{CP} = 12.2 Hz, P*C*H$_2$), 65.1 (vt, J_{CP} = 4.6 Hz, N*C*H$_2$). $^{31}P\{^1H\}$ NMR (161.8 MHz): δ 55.6 (s, *P*^{i}Pr$_2$).

[Ir(CO)(PNP)] (4^{CO}). KO^{t}Bu (0.009 g, 0.080 mmol) is added to a solution of **3^{CO}-[PF$_6$]** (0.041 g, 0.062 mmol) in THF (5 mL) and stirred for 1 h at rt. The solvent is evaporated *in vacuo* and the residue extracted with pentane, filtered, and evaporated to give a yellow solid. Yield: 0.032 g (0.061 mmol; 98%). Anal. Calcd for $C_{17}H_{36}IrNOP_2$ (524.64): C, 38.92; H, 6.92; N, 2.67. Found: 39.43; H, 6.28; N, 2.38. IR (cm^{-1}): ν = 1908 (CO). NMR (C_6D_6, rt, [ppm]) ^1H NMR (399.78 MHz) δ = 1.02 (dvt, $^3J_{HH}$ = 7.2 Hz, J_{HP} = 7.2 Hz, 12H, CH_3), 1.23 (dvt, $^3J_{HH}$ = 8.8 Hz, J_{HP} = 6.8 Hz, 12H, CH_3), 1.81 (tt, $^3J_{HH}$ = 6.6 Hz, J_{HP} = 4.4 Hz, 4H, PCH_2), 1.97 (spvt, $^3J_{HH}$ = 7.0 Hz, J_{HP} = 3.0 Hz, 4H, CH(CH$_3$)$_2$), 3.32 (tvt, $^3J_{HH}$ = 6.4 Hz, J_{HP} = 8.8 Hz, 4H, NCH_2). $^{13}C\{^1H\}$ NMR (100.6 MHz): δ = 18.2 (s, *C*H$_3$), 19.5 (s, *C*H$_3$), 26.2 (vt, J_{CP} = 15 Hz, *C*H(CH$_3$)$_2$), 27.1 (vt, J_{CP} = 13 Hz, P*C*H$_2$), 63.0 (vt, J_{CP} = 5.0 Hz, N*C*H$_2$), 187.8 (t, $^2J_{CP}$ = 9.0 Hz, *C*O). $^{31}P\{^1H\}$ NMR (161.8 MHz): δ 80.7 (s, *P*^{i}Pr$_2$).

[IrHCl$_2$(PNP)^H] (5). HN(CH$_2$CH$_2$P^{i}Pr$_2$)$_2$ (0.102 g; 0.339 mmol) is added to a solution of **1** (0.147 g; 0.164 mmol) in benzene (10 mL) and stirred overnight. The solvent is evaporated *in vacuo* and the residue washed with pentanes to give a white solid, which is dried *in vacuo*. Yield: 0.092 g (0.162 mmol; 49%). Anal. Calcd for $C_{16}H_{38}Cl_2IrNP_2$ (569.55): C, 33.74; H, 6.72; N, 2.46. Found: 33.23; H, 6.59; N, 2.22. IR (cm^{-1}): ν = 3130 (N−H), 2195 (Ir−H). NMR (C_6D_6, rt, [ppm]) ^1H NMR (399.8 MHz): δ −24.73 (t, $^2J_{HP}$ = 12.8 Hz, 1H, IrH), 0.97 (dvt, $^3J_{HH}$ = 7.6 Hz, J_{PH} = 6.8 Hz, 6H, CH_3), 1.11 (dvt, $^3J_{HH}$ = 6.8 Hz, J_{PH} = 6.8 Hz, 6H, CH_3), 1.42 (m, 12H, CH_3, PCH_2, NCH_2), 1.78 (dvt, 6H, $^3J_{HH}$ = 7.6 Hz, J_{PH} = 7.6 Hz, CH_3), 1.99 (m, 2H, CH(CH$_3$)$_2$), 2.56 (m, 2H, CH(CH$_3$)$_2$), 3.27 (m, 2H, NCH_2), 5.11 (br, 1H, NH). $^{13}C\{^1H\}$ NMR (100.6 MHz): δ 17.9 (s, *C*H$_3$), 19.0 (s, *C*H$_3$), 19.4 (s, *C*H$_3$), 20.1 (s, *C*H$_3$), 24.2 (vt, J_{CP} = 13.7 Hz, *C*H(CH$_3$)$_2$), 25.9 (vt, J_{CP} = 13.8 Hz, *C*H(CH$_3$)$_2$), 29.4 (vt, J_{CP} = 12.2 Hz, P*C*H$_2$), 59.3 (s, N*C*H$_2$). $^{31}P\{^1H\}$ NMR (161.8 MHz): δ 27.1 (s, *P*^{i}Pr$_2$).

Reaction of 3^{COE}-PF$_6$ with [PPh$_4$]Cl: NMR Characterization of 6. A suspension of **3^{COE}-PF$_6$** (0.016 g; 0.021 mmol) and [PPh$_4$]Cl (0.008 g, 0.021 mmol) in THF (2 mL) is stirred at room temperature for 36 h, resulting in a mixture of **4^{COE}**, **5**, and **6** by ^{31}P NMR. After evaporation of the solvent the residue is extracted with pentanes and filtered. Upon evaporation of the extract, a mixture of **4^{COE}** and **6** is obtained, which could not be further separated. NMR data of [IrHCl(C$_8$H$_{13}$)(PNP)^H] (**6**): ^1H NMR (399.78 MHz, C_6D_6): δ −24.40 (t, $^2J_{HP}$ = 15.0 Hz, 1H, IrH), 0.95 (dvt, $^3J_{HH}$ = 6.4 Hz, J_{PH} = 6.4 Hz, 6H, CH_3), 1.21 (m, 12H, CH_3), 1.34 (dvt, $^3J_{HH}$ = 6.6 Hz, J_{PH} = 6.6 Hz, 6H, CH_3), 1.53 (m, 2H, NCH_2), 1.67 (m, 4H, PCH_2, CH_2^{COE}), 1.82 (m, 4H, CH_2^{COE}), 1.96 (m, 2H, CH_2^{COE}), 2.11 (m, 2H, CH(CH$_3$)$_2$), 2.40 (m, 6H, PCH_2, NCH_2, IrC=CHCH_2), 3.08 (t, $^3J_{HH}$ = 6.0 Hz, 2H, IrCCH_2), 3.20 (m, 2H, CH(CH$_3$)$_2$), 4.00 (br, 1H, NH), 6.06 (t, $^3J_{HH}$ = 7.7 Hz, 1H, =CH).$^{13}C\{^1H\}$ NMR (100.6 MHz): δ 18.8 (s, *C*H$_3$), 19.1 (s, *C*H$_3$),

19.5 (s, CH_3), 20.0 (s, CH_3), 24.5 (vt, J_{CP} = 13.4 Hz, $CH(CH_3)_2$), 25.7 (vt, $^1J_{CP}$ = 12.2 Hz, $CH(CH_3)_2$), 27.3 (s, CH_2^{COE}), 27.7 (s, CH_2^{COE}), 28.5 (s, CH_2^{COE}) 29.7 (s, CH_2^{COE}), 31.2 (s, IrC=CHCH_2), 31.6 (s, PCH_2), 41.0 (s, IrCCH_2), 54.1 (s, NCH_2), 124.0 (t, $^2J_{CP}$ = 9.2 Hz, IrC), 134.7 (s, IrC=CH). $^{31}P\{^1H\}$ NMR (161.8 MHz): δ 24.4 (s). Assignments were confirmed by $^1H-^1H$ COSY and $^1H-^{13}C$ HSQC spectra.

[IrHCl(COE)(PNP)^H][PF$_6$] (7-PF$_6$). HCl (0.1 M in Et_2O; 0.50 mL; 0.05 mmol) is added to a suspension of **3^{COE}-PF$_6$** (0.038 g; 0.050 mmol) in toluene (3 mL) at −20 °C. After 1 h the solution is filtered at −20 °C and the product precipitated by addition of pentanes to give colorless **7-PF$_6$**. Yield: 0.016 g (20 μmol; 40%). NMR (C_6D_6, rt, [ppm]) ^1H NMR (399.8 MHz): δ −17.83 (t, $^2J_{HP}$ = 10.8 Hz, 1H, IrH), 0.69 (dvt, $^3J_{HH}$ = 6.7 Hz, J_{PH} = 6.7 Hz, 6H, CH_3), 0.75 (dvt, $^3J_{HH}$ = 7.0 Hz, J_{PH} = 7.0 Hz, 6H, CH_3), 0.79 (dvt, $^3J_{HH}$ = 7.0 Hz, J_{PH} = 7.3 Hz, 6H, CH_3), 1.05 (dvt, $^3J_{HH}$ = 8.9 Hz, J_{PH} = 7.6 Hz, 6H, CH_3), 1.12−1.34 (m, 8H, CH_2^{COE}), 1.45 (m, 2H, CH(CH_3)$_2$), 1.47 (m, 2H, NCH_2), 1.57 (m, 2H, CH_2^{COE}), 1.87 (m, 2H, PCH_2), 1.64 (m, 4H, CH_2^{COE}), 2.33 (m, 2H, CH_2^{COE}), 2.80 (m, 2H, PCH_2), 2.89−3.09 (m, 4H, CH(CH_3)$_2$ + NCH_2), 4.06 (br, 2H, CH^{COE}), 5.67 (br, 1H, NH). $^{31}P\{^1H\}$ NMR (161.8 MHz): δ 23.3 (s, P^iPr_2), −142.5 (sp, $^1J_{PF}$ = 707 Hz, PF_6). Assignments were confirmed by $^1H-^1H$ COSY NMR.

Kinetic Experiments. Equimolar amounts (20.2 μmol) of **3^{COE}-PF$_6$** and [N^{n}Bu$_3$(CH_2Ph)]Cl were dissolved in THF (0.35 mL) in a J-Young NMR tube equipped with a sealed capillary of phosphoric acid as internal standard. The reaction was followed recording $^{31}P\{^1H\}$ NMR spectra every 10 min in the inverse-gated mode to avoid NOE buildup. The relaxation delay (15 s) was chosen as $>5T_1$, as derived by ^{31}P NMR inversion recovery experiments of pure samples. Data analysis was performed using the program package COPASI.[47]

X-ray Crystal-Structure Determinations. General. Crystal data and details of the structure determination are presented in Table 4. Suitable single crystals for the X-ray diffraction studies were grown by diffusion of pentane into THF solutions (**3^{C2H4}-PF$_6$**, **3^{CO}-PF$_6$**, **5**) or slow cooling of saturated pentane solutions to −35 °C (**4^{C2H4}**, **4^{CO}**). Crystals were stored under perfluorinated ether, transferred in a Lindemann capillary, fixed, and sealed. Preliminary examinations and data collection were carried out with area detecting systems and graphite-monochromated Mo Kα radiation (λ = 0.71073 Å). The unit cell parameters were obtained by full-matrix least-squares refinements during the scaling procedures. Data collection was performed at low temperatures (Oxford Cryosystems), and each crystal measured with a couple of data sets in rotation scan modus with either $\Delta\varphi/\Delta\omega$ = 1.0° or 2.0°. Intensities were integrated and the raw data were corrected for Lorentz, polarization, and, arising from the scaling procedure, latent decay and absorption effects. The structures were solved by a combination of direct methods and difference Fourier syntheses. All non-hydrogen atoms were refined with anisotropic displacement parameters. Full-matrix least-squares refinements were carried out by minimizing $\sum w(F_o - F_c^2)^2$ with the SHELXL-97 weighting scheme and stopped at shift/err < 0.002. The final residual electron density maps showed no remarkable features. Neutral atom scattering factors for all atoms and anomalous dispersion corrections for the non-hydrogen atoms were taken from International Tables for Crystallography. All calculations were performed on an Intel Pentium 4 PC, with the WinGX system, including the programs PLATON, SIR92, and SHELXL-97.[48]

(47) Hoops, S.; Sahle, S.; Gauges, R.; Lee, C.; Pahle, J.; Simus, N.; Singhal, M.; Xu, L.; Mendes, P.; Kummer, U. *Bioinformatics* **2006**, *22*, 3067.

Specific Details: 3^{C2H4}-PF$_6$: An empirical absorption correction was performed using the PLATON DELABS procedure (T_{min} = 0.116, T_{max} = 0.372). The amine and ethylene hydrogen positions could be located from difference Fourier syntheses and were allowed to refine freely. All other hydrogen atoms were placed in calculated positions and refined using a riding model (d_{C-H} = 0.98, 0.99, and 1.00 Å and $U_{iso(H)} = 1.2U_{eq(C)}$ or $1.5U_{eq(C)}$). **3^{CO}-PF$_6$**: All hydrogen atoms were placed in calculated positions and refined using a riding model (d_{C-H} = 0.98, 0.99, and 1.00 Å, d_{N-H} 0.93 Å, and $U_{iso(H)} = 1.2U_{eq(C/N)}$ or $1.5U_{eq(C)}$). **4^{C2H4}**: A numerical absorption correction after crystal shape optimization was performed using the programs XSHAPE and XRED (T_{min} = 0.157, T_{max} = 0.470). Twinning and the overall crystal quality required setting the resolution limit to 0.93 Å. All hydrogen atoms were placed in calculated positions and refined using a riding model (d_{C-H} = 0.98, 0.99, and 1.00 Å and $U_{iso(H)} = 1.2U_{eq(C)}$ or $1.5U_{eq(C)}$). **4^{CO}**: A numerical absorption correction after crystal shape optimization was performed using the programs XSHAPE and XRED (T_{min} = 0.228, T_{max} = 0.769). All hydrogen atoms were placed in calculated positions and refined using a riding model (d_{C-H} = 0.98, 0.99, and 1.00 Å and $U_{iso(H)} = 1.2U_{eq(C)}$ or $1.5U_{eq(C)}$). Two crystallographic independent molecules were found in the unit cell. **5**: The hydride hydrogen positions could be located from difference Fourier syntheses and were allowed to refine freely. All other hydrogen atoms were placed in calculated positions and refined using a riding model (d_{C-H} of 0.98, 0.99, and 1.00 Å, d_{N-H} 0.93 Å, and $U_{iso(H)} = 1.2U_{eq(C/N)}$ or $1.5U_{eq(C)}$). Two crystallographically independent molecules were found in the unit cell. Crystallographic data (excluding structure factors) for the structures reported in this paper have been deposited with the Cambridge Crystallographic Data Centre as supplementary publication no. CCDC-715654 (**3^{C2H4}-PF$_6$**), CCDC-715652 (**3^{CO}-PF$_6$**), CCDC-715655 (**4^{C2H4}**), CCDC-715653 (**4^{CO}**), and CCDC-715651 (**5**). Copies of the data can be obtained free of charge on application to CCDC, 12 Union Road, Cambridge CB2 1EZ, UK (fax: (+44)1223-336-033; e-mail: deposit@ccdc.cam.ac.uk).

Acknowledgment. The authors thank Prof. W. A. Herrmann for generous support and G. Kummerlöwe and P. Kaden for recording ^{15}N NMR spectra. S.S. is grateful to the DFG for a grant within the Emmy-Noether Programm (SCHN950/2-1), and R.G. would like to thank the Alexander von Humboldt Foundation for a fellowship.

Supporting Information Available: 2D NMR spectra, kinetic fit results, and crystallographic information for complexes **3^{COE}-BPh$_4$**. This material is available free of charge via the Internet at http://pubs.acs.org.

OM800423U

(48) (a) Data Collection Software and Data Processing Software for Stoe IPDS 2T diffractometer, *X-ARERA*, Version 1.26; Stoe & Cie: Darmstadt, Germany, 2004. (b) Data Processing Software for Stoe IPDS 2T diffractometer, *XRED*, *XSHAPE*, Version 1.26; Stoe & Cie: Darmstadt, Germany, 2004. (c) CrysAlis Data Collection Software and Data Processing Software for Oxford Xcalibur diffractometer, Version 1.171; Oxford Diffraction Ltd.: Oxfordshire, U.K., 2005. (d) Farrugia, L. J. WinGX (Version 1.70.01 January 2005). *J. Appl. Crystallogr.* **1999**, *32*, 837−838. (e) Altomare, A.; Cascarano, G.; Giacovazzo, C.; Guagliardi, A.; Burla, M. C.; Polidori, G.; Camalli, M. *SIR92. J. Appl. Crystallogr.* **1994**, *27*, 435–436. (g) *International Tables for Crystallography*; Wilson, A. J. C., Ed.; Kluwer Academic Publishers: Dordrecht, The Netherlands, 1992; Vol. C, Tables 6.1.1.4, 4.2.6.8, and 4.2.4.2. (h) Spek, A. L. *PLATON, A Multipurpose Crystallographic Tool*; Utrecht University: Utrecht, The Netherlands, 2001. (i) Sheldrick, G. M. *SHELXL-97*; Universität Göttingen: Göttingen, Germany, 1998.